

Characterizing Mineral Dusts and Other Aerosols from the Middle East—Part 1: Ambient Sampling

Johann P. Engelbrecht, Eric V. McDonald, and John A. Gillies

Desert Research Institute (DRI), 2215 Raggio Parkway, Reno, Nevada 89512-1095, USA

R. K. M. Jayanty

RTI International, Raleigh, North Carolina 27675-9000, USA

Gary Casuccio

RJ Lee Group, Inc., Monroeville, Pennsylvania 15146, USA

Alan W. Gertler

Desert Research Institute, 2215 Raggio Parkway, Reno, Nevada 89512-1095, USA

The purpose of the Enhanced Particulate Matter Surveillance Program was to provide scientifically founded information on the chemical and physical properties of dust collected over a period of approximately 1 year in Djibouti, Afghanistan (Bagram, Khowst), Qatar, United Arab Emirates, Iraq (Balad, Baghdad, Tallil, Tikrit, Taji, Al Asad), and Kuwait (northern, central, coastal, and southern regions). Three collocated low-volume particulate samplers, one each for the total suspended particulate matter, $<10 \mu\text{m}$ in aerodynamic diameter (PM_{10}) particulate matter, and $<2.5 \mu\text{m}$ in aerodynamic diameter ($\text{PM}_{2.5}$) particulate matter, were deployed at each of the 15 sites, operating on a ‘1 in 6’ day sampling schedule. Trace-element analysis was performed to measure levels of potentially harmful metals, while major-element and ion-chemistry analyses provided an estimate of mineral components. Scanning electron microscopy with energy dispersive spectroscopy was used to analyze the chemical composition of small individual particles. Secondary electron images provided information on particle size and shape. This study shows the three main air pollutant types to be geological dust, smoke from burn pits, and heavy metal condensates (possibly from metals smelting and battery manufacturing facilities). Non-dust storm events resulted in elevated trace metal concentrations in Baghdad, Balad, and Taji in Iraq. Scanning-electron-microscopy secondary electron images of individual particles revealed no evidence of freshly fractured quartz grains. In all instances, quartz grains had rounded edges and mineral grains were generally coated by clay minerals and iron oxides.

INTRODUCTION

The purpose of the Enhanced Particulate Matter Surveillance Program (EPMSP; Engelbrecht et al., 2008) was to provide information on the chemical and physical properties of aerosols collected at 15 locations in the Middle East. Results from this program are available to US Department of Defense occupational-health physicians, as well as environmental health professionals, to assist them in assessing potential human health risk from exposure to ambient particulate matter at their Middle

East military bases. In addition, information on dust allows for an assessment of its potential harmful effect on military equipment. Examples of major-element and trace-element chemistry, and other physical properties, are presented.

In total, 3,136 filter samples were collected on a ‘1-in-6’ day schedule, along with one-time bulk (dust and soil) samples (Engelbrecht et al., in press), at each of the 15 sites. Sample media included Teflon[®] membrane and quartz fiber filters for chemical analysis (71 species), and Nuclepore[®] filters for scanning electron microscopy (SEM) and computer-controlled SEM (CCSEM). In order to fully understand mineral dusts, their chemical and physical properties and mineralogical inter-relationships were accurately established. The purpose of the chemical analysis was to determine levels of potentially harmful trace elements such as lead, arsenic, and other metals. The major-element and ion-chemistry analyses provide an estimate

Received 12 June 2008; revised 5 September 2008; accepted 8 September 2008.

Address correspondence to Johann Engelbrecht, Desert Research Institute, 2215 Raggio Parkway, Reno, NV 89512-1095, U.S.A. E-mail: johann@dri.edu

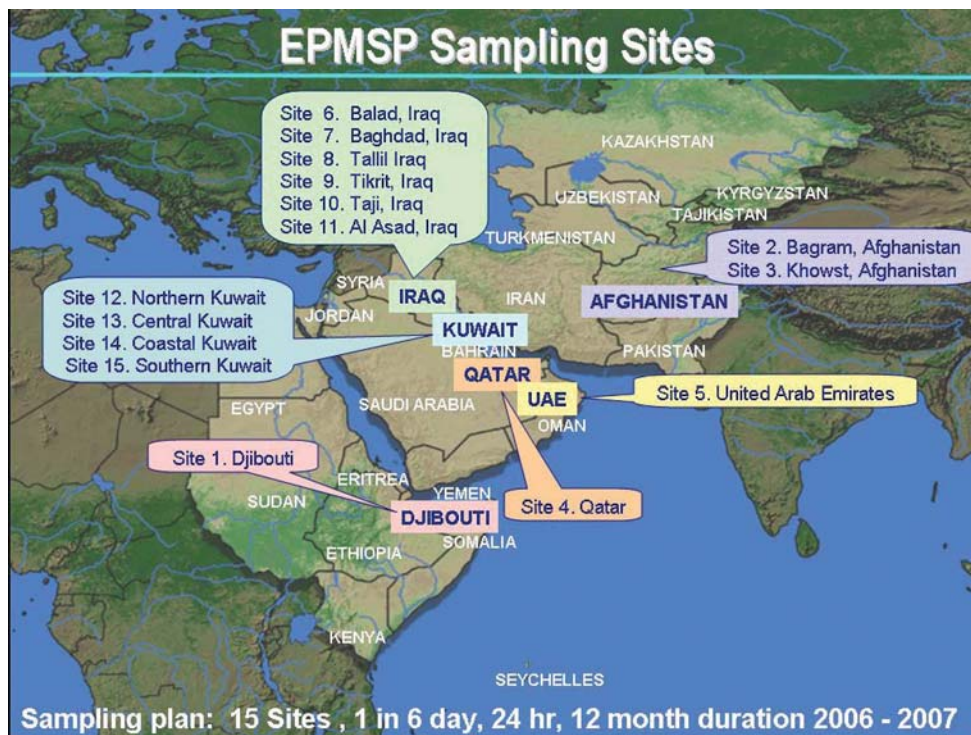


FIG. 1. Map of 15 sampling sites from which ambient aerosol samples were collected over a period of approximately 1 year. Bulk surface-soil samples for re-suspension in the laboratory and analysis were also collected at each site.

of mineral components (e.g. quartz, clays, hematite, evaporates), which themselves may be hazardous to health or else could be carriers of other toxic substances. SEM with energy dispersive spectroscopy (EDS) analyzes the chemical composition of small individual particles of relevance to understanding mineralogical inter-relationships such as surface coatings, intergrowths, and other particle features. Secondary electron images provide information on particle size and shape, which also can be linked to human health effects (e.g. shards of quartz or asbestos fibers that cause physical injuries to lung tissue). The CCSEM is for automated analysis of a large number of individual particles and provides data on individual particle-size distributions and chemical composition.

SAMPLING

Sampling Sites

The 15 sampling localities (Figure 1) were selected to represent areas of potential exposure to military personnel. Sites included were one in Djibouti, two in Afghanistan (Bagram and Khowst), one in Qatar, one in the United Arab Emirates (UAE), six in Iraq (Balad, Baghdad, Tallil, Tikrit, Taji, and Al Asad), and four in Kuwait (northern, central, coastal, and southern regions).

Three criteria were used for selection of the EPMSM sites. The first was the intent to collect air samples from the largest geo-

graphic dispersion within the area of responsibility of the US Central Command. The second was to select locations where US military forces were present, as they are the exposed population of concern for this study. Finally, the sites selected had to have preventive-medicine or military public-health personnel stationed for the duration of the sampling campaign, since they were the scientists, engineers, and technicians responsible for sample collection.

Sampling Equipment and Filter Media

Three sizes of dust samples were collected using collocated low-volume (5 L/min) Airmetrics MiniVol[®] particulate samplers, one each for total suspended (TSP), PM₁₀, and PM_{2.5} particulate matter, deployed at each of the 15 sites. The three samplers were set to start and stop simultaneously, to provide filter sets for comparing the three size fractions.

The filter media (filters) were selected according to the following requirements for each analytical technique:

- The 47 mm diameter Teflon[®] filters were for gravimetry, X-ray fluorescence spectrometry (XRF; 40 elements), and inductively coupled plasma mass spectrometry (ICP-MS; 12 metals).
- The 47 mm diameter quartz fiber filters were for gravimetry, ion chromatography (4 anions, 1 cation), inductively coupled plasma optical emission

TABLE 1

Summary of 1-in-6 day sampling schedule followed at each sampling site in theater. One shipment of 132 exposed filters was lost in transit, but these were replaced by adding sampling days to the end of the original sampling schedule. Analyzed filter days are those for which filter sets were collected for either chemical or computer-controlled scanning electron microscopy (CCSEM) analysis.

Site No.	Site Locality	Site ID	Start	End	Scheduled sampling days	Analyzed filter days
1	Djibouti	DJI-LEM	2005-12-05	2007-06-09	60	70
2	Bagram, Afghanistan	AFG_BAG	2005-12-07	2004-05-21	60	75
3	Khowst, Afghanistan	AFG_SAL	2006-04-28	2007-06-22	60	60
4	Qatar	QAT_UDE	2006-02-16	2007-02-06	60	60
5	United Arab Emirates	UAE_DHA	2006-02-18	2007-02-07	60	60
6	Balad, Iraq	IRQ_ANA	2006-01-15	2007-03-24	60	60
7	Baghdad, Iraq	IRQ_VIC	2006-01-08	2007-01-11	60	58
8	Iraq	IRQ_ADD	2006-01-15	2007-02-15	60	60
9	Tikrit, Iraq	IRQ_SPE	2006-01-12	2007-03-12	60	62
10	Taji, Iraq	IRQ_TAJ	2006-02-05	2007-02-11	60	60
11	Iraq, Al	IRQ_ALA	2006-01-08	2006-12-26	60	56
12	Northern Kuwait	KUW_BUE	2006-01-28	2007-02-04	60	59
13	Central Kuwait	KUW_AAS	2006-03-14	2007-03-19	60	60
14	Coastal Kuwait	KWT_SHU	2006-01-20	2007-03-20	60	61
15	Southern Kuwait	KUW_ARI	2006-01-21	2007-01-15	60	60
Total					900	921

spectrometry (ICP-OES; 4 cations), and thermal optical transmission (3 carbon species).

- The 47 mm diameter Nuclepore[®] filters were for individual particle analysis by SEM (secondary electron images) and CCSEM (28 chemical species).

Sampling Schedule

Three different sample sets were collected on different sampling days, Sample Set T on Teflon membrane filters, Sample Set Q on quartz fiber filters, and Sample Set N on Nuclepore[®] filters.

A 1-in-6 day sampling schedule was essentially followed; however, although the sites did sample at this frequency, not all were sampled on the same sixth day. On each sampling day either Teflon[®], quartz fiber, or Nuclepore[®] filters were used. Over a period of 1 month, there were 2 sampling days each for Teflon[®] and quartz fiber filters, and 1 sampling day for Nuclepore[®] filters. For Nuclepore[®] filters, the sampling period was 2 h, so as to provide lightly loaded filters with dispersed single particles, as required for CCSEM analysis. A summary of sampling days and days for which filters were collected for analyses is in Table 1. The laboratory analyses performed in the course of the EPMSF are summarized in Table 2.

ANALYTICAL PROCEDURES

To fully understand their potential impact on human health, ambient aerosols and re-suspended soils were chemically, physically, and mineralogically characterized.

The Teflon[®] membrane and quartz fiber filters were conditioned and weighed prior to and after sampling, to measure the mass of particulate matter sampled in the field during each 24-hour sampling period¹. From the flow volumes recorded on data sheets in the field and measured mass, particulate matter (PM) concentrations were calculated to micrograms per cubic meter ($\mu\text{g}/\text{m}^3$) of sampled air.

In the course of this study, Teflon[®] filters, including 92 field and 22 laboratory blanks were analyzed by energy dispersive X-ray fluorescence spectrometry (EDXRF) for 40 chemical elements, including sodium, magnesium, aluminum, silicon, phosphorus, sulfur, chlorine, potassium, calcium, titanium, vanadium, chromium, manganese, iron, cobalt, nickel, copper, zinc, gallium, arsenic, selenium, bromine, rubidium, strontium, yttrium, zirconium, molybdenum, palladium, silver, cadmium, indium, tin, antimony, barium, gold, mercury, thallium, lead, lanthanum, and uranium. EDXRF is a non-destructive analytical technique performed on filter samples. After completion and validation of the EDXRF results, the same Teflon[®] filters were dissolved in nitric and hydrochloric acid mixture, and the solutions analyzed by inductively coupled plasma mass spectrometry (ICP-MS) for 12 trace metals: antimony; arsenic; beryllium; cadmium; chromium; lead; manganese; nickel; vanadium; zinc; mercury; and strontium. Water extractions were performed on half of each of the quartz fiber filters, including field and laboratory blanks. Aliquots of the extractions were analyzed by ion chromatography for water soluble anions, sulfate (SO_4^{2-}), nitrate (NO_3^-), chloride (Cl^-), phosphate (PO_4^{3-}), and the ammonium

TABLE 2
Summary of the approximate number of analyses performed on filter media and bulk samples in the course of the study

	Total Samples	Analytical method	Species/parameters analyzed (Est.)	Samples/Particles/ Units	Total analyses (Estimate)
AMBIENT FILTER SAMPLES					
<i>Teflon filters</i>					
Mass	1224	Gravimetric	1	1,224	1,224
Elemental analysis	1224	XRF	40	1,224	48,960
Trace metal analysis	1224	ICP-MS	12	1,224	14,688
<i>Quartz fiber filters</i>					
Mass	1223	Gravimetric	1	1,223	1,223
Soluble anions and ammonium	1223	IC	5	1,223	6,115
Soluble cations	1223	ICP-OES	4	1,223	4,892
Carbon and carbonate	1223	TOT	9	1,223	11,007
<i>Nuclepore filters</i>					
Individual particle analysis 0.5–15 micron	243	CCSEM	28	256,334	7,177,352
Images & spectra	84	SEM	1	84	84
Ultrafines <0.5 micron	15	CCSEM	28	1,558	43,624
				Subtotal	7,309,169
RESUSPENDED DUST SAMPLES					
<i>Teflon filters</i>					
Mass	30	Gravimetric	1	30	30
Elemental analysis	30	XRF	40	30	1,200
Trace metal analysis	30	ICP-MS	12	30	360
<i>Quartz fiber filters</i>					
Mass	30	Gravimetric	1	30	30
Soluble anions	30	IC	4	30	120
Soluble cations	30	AA	4	30	120
Carbon and carbonate	30	TOR	9	30	270
Ammonium	30	AC	1	30	30
<i>Nuclepore filters</i>					
Individual particle analysis	15	CCSEM	28	14,900	417,200
				Subtotal	419,360
BULK DUST SAMPLES					
<i>Soil chemistry</i>					
Hydrogen-ion activity	15	pH	1	15	15
Carbonate content	15	Acid digestion	1	15	15
Electrical conductivity	15	EC	1	15	15
<i>Elemental and minerals analysis</i>					
Elemental analysis	15	XRF	13	15	195
Minerals analysis	15	XRD	12	15	180
<i>Particle-size analysis</i>					
Particle-size distribution (sand, silt, clay)	15	PSD	1	15	15
				Subtotal	435
				Total analyses	7,728,964

Acronym	Analytical Method	Application
AA	Atomic Absorption	Cation analysis
AC	Automated Colorimetry	Ammonium analysis
CCSEM	Computer Controlled Scanning Electron Microscopy	Individual particle size, shape and chemistry (0.5–15 micron)
EC	Electrical Conductivity	Salts in soil
IC	Ion Chromatography	Anion and ammonium analysis
ICP-MS	Inductively Coupled Plasma Mass Spectrometry	Trace metal analysis
ICP-OES	Inductively Coupled Plasma - Optical Emission Spectrometry	Cation analysis
PSD	Particle-size distribution	Particle-size distribution by laser diffraction
SEM	Scanning Electron Microscopy	Secondary electron particle image & XRF spectrum
TOR	Thermal Optical Reflectance	OC, EC and Carbonate analysis
TOT	Thermal Optical Transmission	OC, EC and Carbonate analysis
XRD	X-ray Diffraction	Mineral analysis
XRF	X-Ray Fluorescence Spectrometry	Major elemental analysis

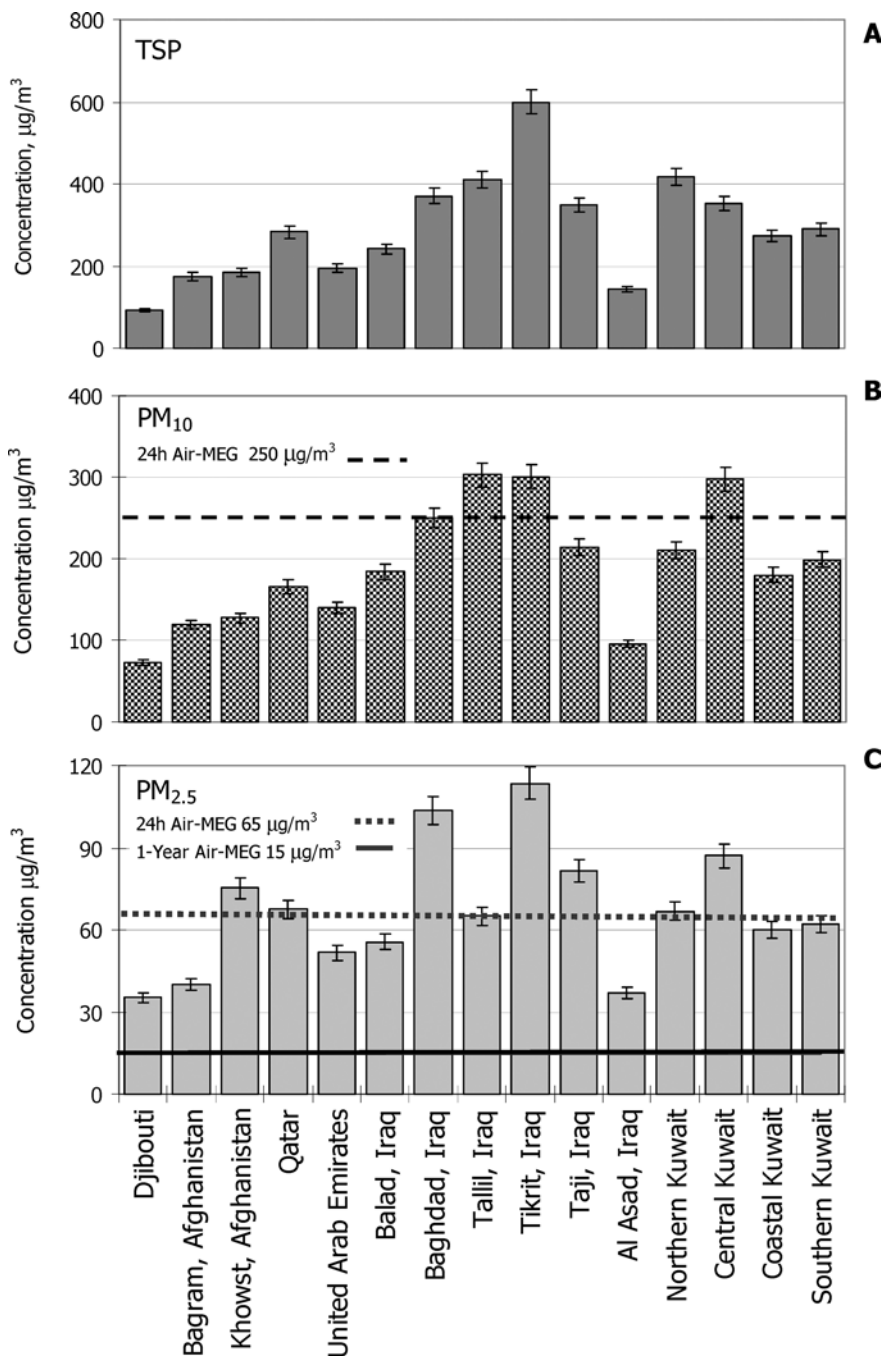


FIG. 2. Averaged particulate mass concentrations and uncertainties for (A) TSP, (B) PM₁₀, and (C) PM_{2.5} on Teflon[®] filters for each of the 15 sites. Averaging period is approximately 1 year. Also shown are the 24 h and 1-year Military Exposure Guidelines (MEGs) for particulate matter.

(NH₄⁺) cation. Further aliquots of the extractions were analyzed by inductively coupled plasma optical emission spectrometry (ICP-OES), for water soluble cations, sodium (Na⁺), potassium (K⁺), calcium (Ca²⁺), and magnesium (Mg²⁺).

Punches from the remaining half of each of the quartz fiber filters were analyzed for organic carbon and elemental carbon

by the NIOSH method.² Separate punches were acidified to dissolve carbonate (CO₃²⁻), and the latter was determined by the difference in total carbon between non-acidified and acidified punches.

SEM individual particle analysis was performed on approximately 258 filters selected from approximately 555 sampled

Nuclepore[®] filters. A dual approach was followed, the first being the CCSEM and the second being secondary electron imaging by high magnification SEM.

CCSEM is a combination of backscattered electron imagery and EDS that automatically analyzes in a cost-effective fashion a large number (1,000–1,500) of individual particles for particle size and chemical composition. The particles are grouped in 'bins' by chemical composition and particle size. From these chemical measurements, the mineralogy of individual particles can be inferred, for example Si particles being quartz and Ca particles being calcite. From each of the 15 sites, at least one TSP, at least four PM_{2.5}, and 3–10 PM₁₀ Nuclepore[®] filters were analyzed by CCSEM. Also, one PM_{2.5} filter from each site was analyzed for its ultrafine (0.01–0.50 μm diameter) individual particle content. Although labor intensive, the field emission electron source of the SEM allows for very high magnification and sharp secondary electron images. This technique is for the study of particle shape, surface coatings, and chemical composition. More than 80 secondary electron images representing all 15 sites were collected in this way.

Upon completion of analysis, filter results underwent a first level of quality assurance, before being uploaded to appropriate folders on the EPMSF webpage by each laboratory. The Desert Research Institute retrieved these files for second-level quality assurance, including data validation, flagging, and compilation into folders for each site. Results were tabulated and graphically displayed as time-series plots, pie-charts, and stacked bar-charts as part of a third level of quality assurance.

Chemical, mineralogical, and electron-microscopy results of all analyzed filter and bulk soil samples for each of the 15 sites were submitted to the US Army Center for Health Promotion and Preventative Medicine (USACHPPM) for archiving, following a final quality-assurance review.

RESULTS

All analytical results for each site—together with statistics, and graphical representations were compiled on spread sheets. Of 2,308 (excluding blanks) Teflon[®] membrane and quartz fiber filters sampled in the field, 2,207 (96%) were chemically analyzed, and after the elimination of voided results, a filter recovery of 2,022 (88%) was provided for subsequent data analysis. The following results include some sites and key chemical species that highlight areas of potential concern to the US Department of Defense.

Gravimetry

Time-series plots for TSP, PM₁₀, and PM_{2.5} 24h gravimetric and chemical abundances from Teflon[®] and quartz fiber filters were compiled for each of the 15 sites. Averaged concentration levels (Figure 2, Table 3) show highest particulate matter concentrations for TSP at Tikrit (605 $\mu\text{g}/\text{m}^3$) and PM₁₀ at Tallil (303 $\mu\text{g}/\text{m}^3$). Differences among sites for PM_{2.5} total mass concentrations are less, with Tikrit giving the highest annual average PM_{2.5} concentration of 111 $\mu\text{g}/\text{m}^3$.

TABLE 3

Mean mass concentrations for TSP, PM₁₀, and PM_{2.5} size fractions, as well as the TSP:PM₁₀:PM_{2.5} mass ratios for each of the 15 sites, as measured on Teflon[®] filters. For comparison, the mean concentrations and ratios from sites in the southwestern urban (CSN) and rural (IMPROVE) US are also given

Site No.	Site location	Concentration ($\mu\text{g}/\text{m}^3$)			Ratio		
		TSP	PM ₁₀	PM _{2.5}	TSP	PM ₁₀	PM _{2.5}
1	Djibouti	92	72	35	1.27	1	0.49
2	Bagram, Afghanistan	174	108	38	1.62	1	0.35
3	Khowst, Afghanistan	184	127	75	1.45	1	0.59
4	Qatar	282	165	67	1.71	1	0.41
5	United Arab Emirates	196	140	52	1.40	1	0.37
6	Balad, Iraq	242	184	56	1.31	1	0.30
7	Baghdad, Iraq	371	250	103	1.48	1	0.41
8	Tallil, Iraq	411	303	65	1.36	1	0.21
9	Tikrit, Iraq	605	298	111	2.03	1	0.37
10	Taji, Iraq	348	213	81	1.63	1	0.38
11	Al Asad, Iraq	142	95	37	1.49	1	0.39
12	Northern Kuwait	416	211	67	1.98	1	0.32
13	Central Kuwait	352	298	87	1.18	1	0.29
14	Coastal Kuwait	268	176	60	1.52	1	0.34
15	Southern Kuwait	290	199	62	1.45	1	0.31
CSN	US SW urban (city)	—	40	12	—	1	0.30
IMPROVE	US SW rural (desert)	—	13	5	—	1	0.36

TABLE 4

Comparative table showing concentration ranges in $\mu\text{g}/\text{m}^3$ of mean $\text{PM}_{2.5}$ site concentrations, as well as various air-quality and health standards

Symbol	Name	Mnemonic	Method	Range of Annual Mean of 15 Sites			Site Ranking			USACHPPM			US EPA		WHO		NIOSH		OSHA	
				$\text{PM}_{2.5}$			Highest	2nd Highest	3rd Highest	8-hour Air-MEG $\mu\text{g}/\text{m}^3$	1-Year Air-MEG $\mu\text{g}/\text{m}^3$	Annual NAAQS $\mu\text{g}/\text{m}^3$	24 hr TWA $\mu\text{g}/\text{m}^3$	Annual NAAQS $\mu\text{g}/\text{m}^3$	10-hr day (10-hr day 40-h workweek) $\mu\text{g}/\text{m}^3$	40-h (8-hr day 40-h workweek) $\mu\text{g}/\text{m}^3$	REL: TWA PEL: TWA	REL: TWA PEL: TWA		
				Min (a)	Max (b)	Annual Mean (c)													(d)	(e)
TSP	TSP Mass Teflon	TMAC	GRAV	92	605	IRQ_SPE	KUW_BUE	IRQ_ADD												
PM_{10}	PM_{10} Mass Teflon	TMAC	GRAV	72	303	KUW_AAS	IRQ_VIC	IRQ_TAJ			150	20								
$\text{PM}_{2.5}$	$\text{PM}_{2.5}$ Mass Teflon	TMAC	GRAV	35	111	IRQ_SPE	IRQ_VIC	KUW_AAS			35	10								
Cl^-	Chloride	CLJC	IC	0.149	0.857	UAE_DHA	IRQ_TAJ	IRQ_ADD	Particulate Matter Mass Concentrations											
NO_3^-	Nitrate	N3IC	IC	0.586	2.064	IRQ_VIC	AFG_BAG	QAT_UDE	$\text{PM}_{2.5}$ Chemical Concentrations											
PO_4^{3-}	Phosphate	PHIC	IC	0.047	0.166	IRQ_VIC	IRQ_ALA	KUW_ARI												
SO_4^{2-}	Sulfate	S4IC	IC	2.138	11.915	KWT_SHU	KUW_ARI	UAE_DHA												
NH_4^+	Ammonium	N4IC	IC	0.865	3.629	KWT_SHU	KUW_ARI	KUW_AAS												
Ca^{2+}	Calcium	CAEC	ICP-OES	0.247	3.555	IRQ_VIC	IRQ_SPE	IRQ_ALA												
K^+	Potassium	KPEC	ICP-OES	0.086	0.250	IRQ_TAJ	AFG_SAL	IRQ_VIC												
Mg^{2+}	Magnesium	MGEC	ICP-OES	0.036	0.260	KUW_AAS	UAE_DHA	IRQ_VIC												
Na^+	Sodium	NAEC	ICP-OES	0.057	0.310	UAE_DHA	DJLLEM	IRQ_VIC												
$\text{CO}_3(\text{C})$	Carbonate carbon	C3TC	TOT	0.855	2.241	IRQ_VIC	IRQ_ALA	IRQ_SPE												
C	Elemental carbon	ECTNIC	TOT	1.152	5.085	KUW_ARI	KWT_SHU	IRQ_SPE												5000
OC	Organic carbon	OCTNIC	TOT	1.373	9.864	AFG_BAG	AFG_SAL	IRQ_TAJ												
TOC	Total carbon	TCTC	TOT	3.400	14.543	IRQ_VIC	AFG_SAL	AFG_BAG												
Ag	Silver	AGXC	XRF	0.009	0.016	IRQ_SPE	AFG_SAL	DJLLEM												
Al	Aluminum	ALXC	XRF	0.465	3.207	IRQ_SPE	KUW_AAS	IRQ_VIC												
As	Arsenic	ASXC	XRF	0.002	0.056	IRQ_VIC	IRQ_TAJ	IRQ_ANA												
Au	Gold	AUXC	XRF	0.003	0.016	AFG_SAL	DJLLEM	IRQ_VIC												
Ba	Barium	BAXC	XRF	0.007	0.066	IRQ_VIC	KUW_AAS	OAT_UDE												
Br	Bromine	BRXC	XRF	0.003	0.019	IRQ_VIC	IRQ_ANA	KUW_ARI												
Ca	Calcium	CAXC	XRF	0.549	6.481	IRQ_VIC	IRQ_SPE	KUW_AAS												
Cd	Cadmium	CDXC	XRF	0.011	0.020	IRQ_SPE	KUW_ARI	DJLLEM												
Cl	Chlorine	CLXC	XRF	0.041	0.799	IRQ_VIC	DJLLEM	IRQ_TAJ												
Co	Cobalt	COXC	XRF	0.001	0.001	IRQ_SPE	IRQ_TAJ	KUW_ARI												
Cr	Chromium	CRXC	XRF	0.001	0.002	IRQ_SPE	IRQ_TAJ	KUW_ARI												
Cu	Copper	CUXC	XRF	0.001	0.010	IRQ_VIC	IRQ_ANA	KWT_SHU												
Fe	Iron	FEXC	XRF	0.420	2.847	IRQ_SPE	KUW_AAS	IRQ_VIC												
Ga	Gallium	GAXC	XRF	0.002	0.007	IRQ_VIC	IRQ_SPE	IRQ_TAJ												

Hg	Mercury	HGXC	XRF	0.005	0.010	IRQ_SPE	AFG_SAL	IRQ_TAJ	0.205	1	10	10
In	Indium	INXC	XRF	0.015	0.029	IRQ_SPE	AFG_SAL	IRQ_TAJ			100	100
K	Potassium	KPXC	XRF	0.211	1.074	IRQ_VIC	IRQ_SPE	IRQ_TAJ				
La	Lanthanum	LAXC	XRF	0.005	0.060	IRQ_VIC	KUW_AAS	KUW_BUE				
PM2.5 Chemical Concentrations												
Ma	Magnesium	MGXC	XRF	0.175	1.486	IRQ_SPE	KUW_AAS	IRQ_VIC		0.15	1000	
Mn	Manganese	MNXC	XRF	0.006	0.047	IRQ_SPE	IRQ_VIC	KUW_AAS	0.342			
Mo	Molybdenum	MOXC	XRF	0.006	0.010	IRQ_SPE	IRQ_TAJ	KUW_ARI				10000
Na	Sodium	NAXC	XRF	0.111	0.496	IRQ_VIC	DJLLEM	UAE_DHA				
Ni	Nickel	NIXC	XRF	0.002	0.012	AFG_SAL	IRQ_SPE	IRQ_VIC	4.9			1000
P	Phosphorus	PHXC	XRF	0.034	0.323	IRQ_SPE	IRQ_VIC	KUW_AAS				
Pb	Lead	PBXC	XRF	0.005	0.581	IRQ_VIC	IRQ_TAJ	IRQ_ANA	1.5	0.5	50	50
Pd	Palladium	PDXC	XRF	0.007	0.013	IRQ_SPE	DJLLEM	IRQ_TAJ				
Rb	Rubidium	RBXC	XRF	0.002	0.005	IRQ_SPE	IRQ_TAJ	AFG_SAL				
S	Sulfur	SUXC	XRF	0.671	3.727	QAT_UDE	UAE_DHA	KUW_BUE				
Sb	Antimony	SBXC	XRF	0.027	0.074	IRQ_ANA	IRQ_SPE	DJLLEM	12		500	500
Se	Selenium	SEXC	XRF	0.001	0.003	IRQ_SPE	IRQ_VIC	IRQ_TAJ			200	200
Si	Silicon	SIXC	XRF	1.182	8.876	IRQ_SPE	KUW_AAS	IRQ_VIC			5000	5000
Sn	Tin	SNXC	XRF	0.022	0.037	IRQ_SPE	IRQ_VIC	OAT_UDE			2000	2000
Sr	Strontium	SRXC	XRF	0.004	0.030	UAE_DHA	IRQ_VIC	OAT_UDE				
Ti	Titanium	TTXC	XRF	0.017	0.155	KUW_AAS	IRQ_SPE	AFG_SAL				
Tl	Thallium	TLXC	XRF	0.003	0.006	IRQ_VIC	IRQ_SPE	IRQ_TAJ	1510			
U	Uranium	URXC	XRF	0.021	0.037	IRQ_SPE	IRQ_TAJ	KUW_ARI			200	250
V	Vanadium	VAXC	XRF	0.012	0.107	IRQ_VIC	IRQ_SPE	KUW_AAS	0.72		1000	500
Y	Yttrium	YTXC	XRF	0.002	0.003	IRQ_SPE	IRQ_TAJ	KUW_AAS				1000
Zn	Zinc	ZNXC	XRF	0.014	0.043	IRQ_TAJ	IRQ_VIC	KWT_SHU	720			
Zr	Zirconium	ZRXC	XRF	0.003	0.011	IRQ_VIC	IRQ_SPE	KUW_AAS			5000	5000
As	Arsenic	ASMC	ICP-MS	0.002	0.004	IRQ_VIC	IRQ_SPE	IRQ_TAJ	1.11		10	10
Be	Beryllium	BEMC	ICP-MS	0.000	0.001	IRQ_SPE	IRQ_TAJ	KUW_ARI	0.014		2	2
Cd	Cadmium	CDMC	ICP-MS	0.000	0.002	IRQ_ANA	IRQ_VIC	IRQ_TAJ	0.244	0.005		5
Cr	Chromium	CRMC	ICP-MS	0.003	0.013	IRQ_SPE	AFG_SAL	KUW_AAS	12.20			

(Continued on next page)

TABLE 4

Comparative table showing concentration ranges in $\mu\text{g}/\text{m}^3$ of mean $\text{PM}_{2.5}$ site concentrations, as well as various air-quality and health standards (Continued)

Symbol	Name	Mnemonic	Method	Range of Annual Mean of 15 Sites			Site Ranking			USACHPPM		US EPA	WHO	NIOSH	OSHA	
				Min	Max	3rd Highest	2nd Highest	Highest	8-hour Air-MEG	1-Year Air-MEG	Annual NAAQS	24 hr TWA	TWA	(10-hr day)	REL: TWA	PEL: TWA
				(a)	(b)	(c)	(d)	(e)	(f)	(g)	(h)	(i)	(j)	(k)	(l)	(m)
Hg	Mercury	HGMC	ICP-MS	0.000	0.001	IRQ_SPE	IRQ_ADD	UAE_DHA		0.205		1	10	10		
Mn	Manganese	MNMC	ICP-MS	0.011	0.055	IRQ_SPE	KUW_AAS	AFG_SAL		0.342		0.15	1000			
Ni	Nickel	NIMC	ICP-MS	0.002	0.014	AFG_SAL	IRQ_SPE	IRQ_VIC		36.7				1000		
Pb	Lead	PBMC	ICP-MS	0.007	0.546	IRQ_VIC	IRQ_TAJ	IRQ_ANA		1.5	1.5	0.5	50	50		
Sb	Antimony	SBMC	ICP-MS	0.001	0.050	IRQ_ANA	IRQ_VIC	AFG_BAG		12			500	500		
Sr	Strontium	SRMC	ICP-MS	0.002	0.019	QAT_UDE	IRQ_VIC	UAE_DHA		1510						
V	Vanadium	VAMC	ICP-MS	0.001	0.009	IRQ_SPE	IRQ_VIC	KWT_SHU		0.72				500		
Zn	Zinc	ZNMC	ICP-MS	0.028	0.069	IRQ_TAJ	KWT_SHU	IRQ_ANA		720						

(a) and (b) The range in annual mean concentration values among the 15 sites. Mean concentrations calculated for each chemical species and each site on the $\text{PM}_{2.5}$ size fraction unless stated otherwise.

(c), (d) and (e) Three sites with the highest, second highest, and third highest annual mean concentration per species. Site mnemonics are (1) DJLLEM = Djibouti, (2) AFG_BAG = Afghanistan Bagram, (3) AFG_SAL = Afghanistan Khowst, (4) QAT_UDE = Qatar, (5) UAE_DHA = United Arab Emirates, (6) IRQ_ANA = Iraq Balad, (7) IRQ_VIC = Iraq Baghdad (8) IRQ_ADD = Iraq Tallil, (9) IRQ_SPE = Iraq Tikrit, (10) IRQ_TAJ = Iraq Taji, (11) IRQ_ALA = Iraq Al Asad, (12) KUW_BUE = Northern Kuwait, (13) KUW_AAS = Central Kuwait, (14) KWT_SHU = Coastal Kuwait, (15) KUW_ARI = Southern Kuwait

(f) and (g) USACHPPM 8-hour and 1-year Air-MEGs: USACHPPM Military Exposure Guidelines (MEG) for Deployed Military Personnel, Tabel 1. Military Exposure Guidelines for Air - January 2004 TG 230 Addendum (<http://chppm-www.apgea.army.mil/documents/TG/TECHGUID/TG230.pdf>) revised July 2008 (http://chppm-www.apgea.army.mil/documents/FACT/Particulate%20Matter_Factsheet_2008_30%20July_08_final.pdf).

(h) and (i) US EPA NAAQS: United States Environmental Protection Agency Ambient Air Quality Standards, 1 year and 24 h (<http://www.epa.gov/air/criteria.html>).

(j) WHO TWA annual: World Health Organization (WHO) annual time-weighted average (TWA), Air quality guidelines - global update 2005, http://www.who.int/phe/health_topics/outdoorair_aqg/en/index.html

(k) NIOSH REL TWA: National Center for Disease Control (CDC), National Institute for Occupational Safety and Health (NIOSH), recommended exposure limit (REL), 10-hour time-weighted average (TWA), 40-hour workweek (<http://www.cdc.gov/niosh/npg/npgd0022.html>), INDEX of Chemical Abstracts Service Registry Numbers (CAS No.) (<http://www.cdc.gov/niosh/npg/npgdcas.html>).

(l) OSHA PEL TWA: Occupational Safety and Health Administration standards, permissible exposure limit (PEL), time-weighted average (TWA) 8-hour day, Regulations (Standards - 29 CFR), TABLE Z-1, Limits for Air Contaminants (http://www.osha-slc.gov/pls/oshaweb/owadisp.show_document?p_table=STANDARDS&p_id=9992).

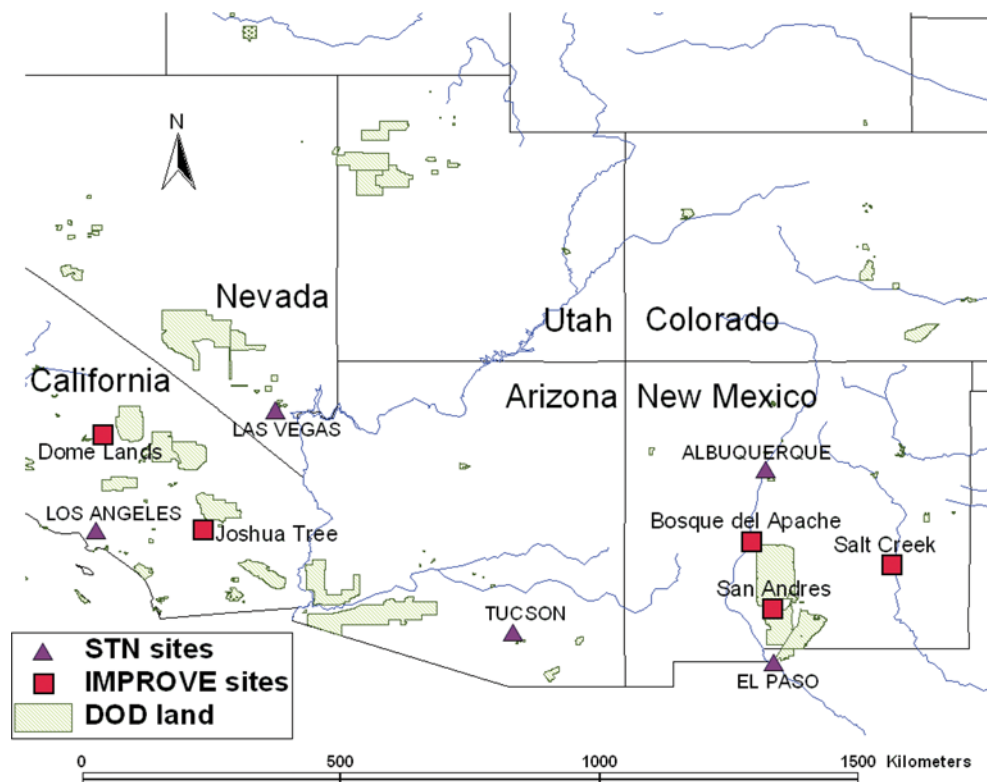


FIG. 3. Location of Department of Defense (DOD) lands in the southwestern US in relation to five rural IMPROVE sites (Dome Land National Wildlife Area, Joshua Tree National Park, Bosque del Apache National Wildlife Reserve, Salt Creek, and San Andres National Wildlife Reserve) and five urban Chemical Speciation Network (STN) sites (Las Vegas, Los Angeles, Tucson, Albuquerque, and El Paso).

Although both Teflon[®] and quartz fiber filters were weighed, gravimetric results from the latter were often found to be less reliable. This is due to the brittle nature of the glass fiber filter medium and subsequent loss of mass from small bits of fiber breaking off edges of the filters. In some instances, this was negligible but, in other cases, it resulted in underestimation of the PM mass collected on quartz fiber filters.

The high average particulate matter (TSP, PM₁₀, and PM_{2.5}) levels from each site are to a large extent determined by the number and intensity of dust-blowing events. Differences in PM measurements among Baghdad, Taji, Balad, and Tikrit (all within 200 km of each other along the Tigris River valley) can be ascribed to varying contributions from local dust sources, including dirt and paved roads, agriculture, and disturbances of the desert floor by motorized vehicles.

The PM_{2.5}:PM₁₀ mass ratios vary substantially among the 15 sites, from 0.21 for Tallil, Iraq to 0.59 for Khowst, depending on the fraction of coarse dust in the air. For the Iraq and Kuwait sites, the average PM_{2.5}:PM₁₀ mass ratio is 0.33, which is slightly less than the average ratio of 0.36 for the rural southwestern area of the US (Table 3). This signifies that, on average, the PM_{2.5}:PM₁₀ particulate mass distribution of sampled areas in the Middle East is similar to that of the drier parts of the

southwestern area of the US. This low value is typical of regions dominated by geological dust, in contrast to rural areas, where combustion processes such as coal or wood burning dominate (Engelbrecht et al., 2001), and where the PM_{2.5}:PM₁₀ ratios are on average as high as 0.85.

Although no longer monitored in the US or considered a health standard, TSP was measured as part of the EPMS because of the impact of coarse dust on military equipment. Average TSP:PM₁₀ mass ratios vary from 1.18 for Central Kuwait to as high as 2.03 for Tikrit, Iraq, emphasizing dominance by coarse dust at the latter site.

Air Quality and Health Standards

Table 4 provides a summary of concentration levels measured in the course of the EPMS, as well as US and international health standards. It should be noted that the air-quality standards listed in this table have qualifiers regarding the way in which samples are to be collected, analytical methods are to be applied, as well as which chemical species to be considered or excluded. References for each air-quality and health standard are listed as a footnote to Table 4. For this study, tabled values serve as indicators only. Because of health risks associated with

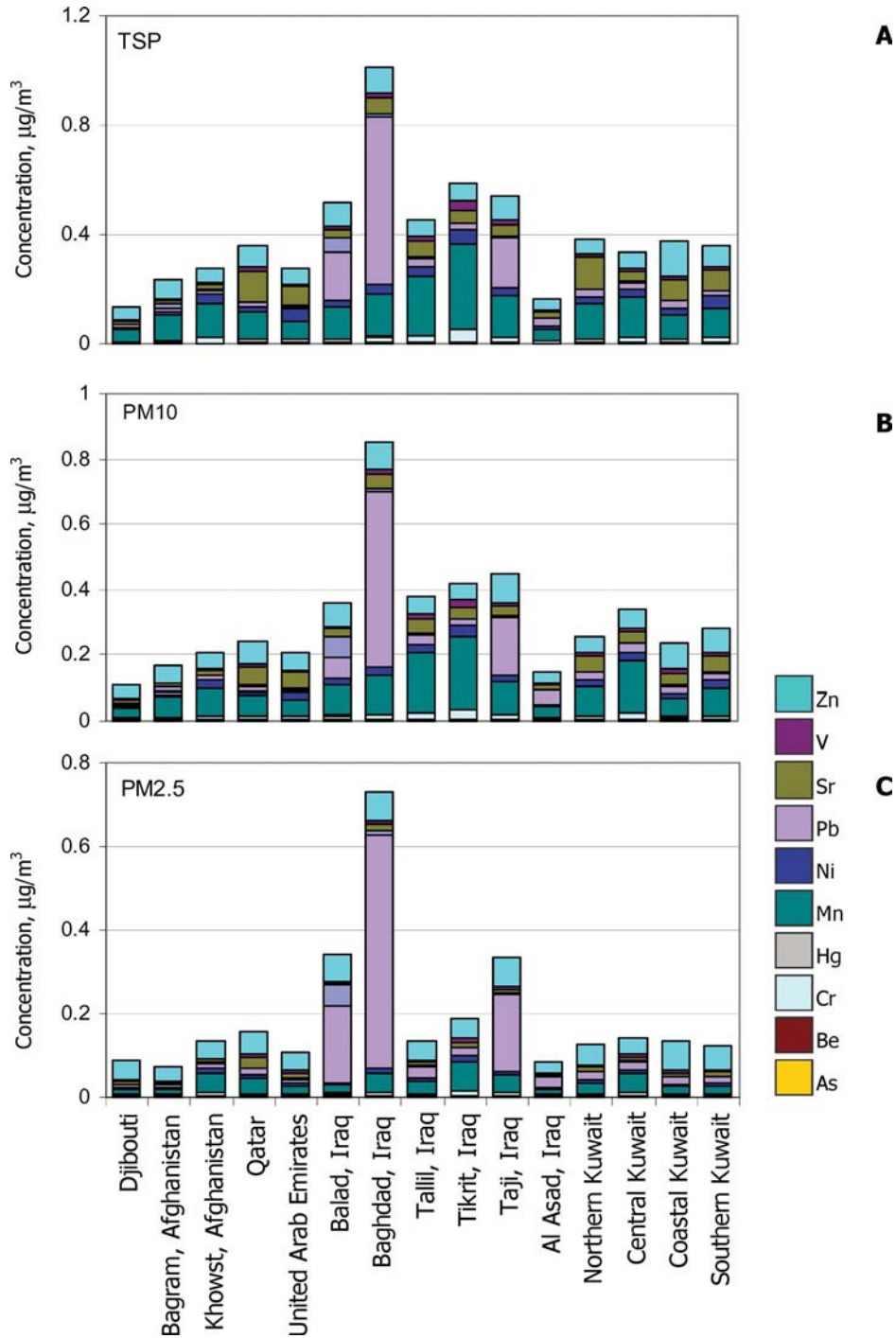


FIG. 4. Annual mean distributions of 12 trace metals for (A) TSP, (B) PM_{10} , and (C) $PM_{2.5}$ size fractions for each of the 15 sites.

the finer fraction, only $PM_{2.5}$ levels are presented in this document. It will be shown that trace metals—such as lead, arsenic, cadmium, antimony, and zinc—are concentrated in the $PM_{2.5}$ fraction (Figures 4–6 and 10B). Also, fine aluminum silicate minerals such as clays are generally concentrated in the fine fraction.

When results are averaged for the sampling period of approximately 1 year, all sites exceed the USACHPPM 1-year air Military Exposure Guideline (MEG) value of $15 \mu\text{g}/\text{m}^3$ for $PM_{2.5}$. Other standards that were exceeded are the World Health Organization (WHO)'s guidelines for particulate matter ($20 \mu\text{g}/\text{m}^3$ for PM_{10} , $10 \mu\text{g}/\text{m}^3$ for $PM_{2.5}$). It is of note that the

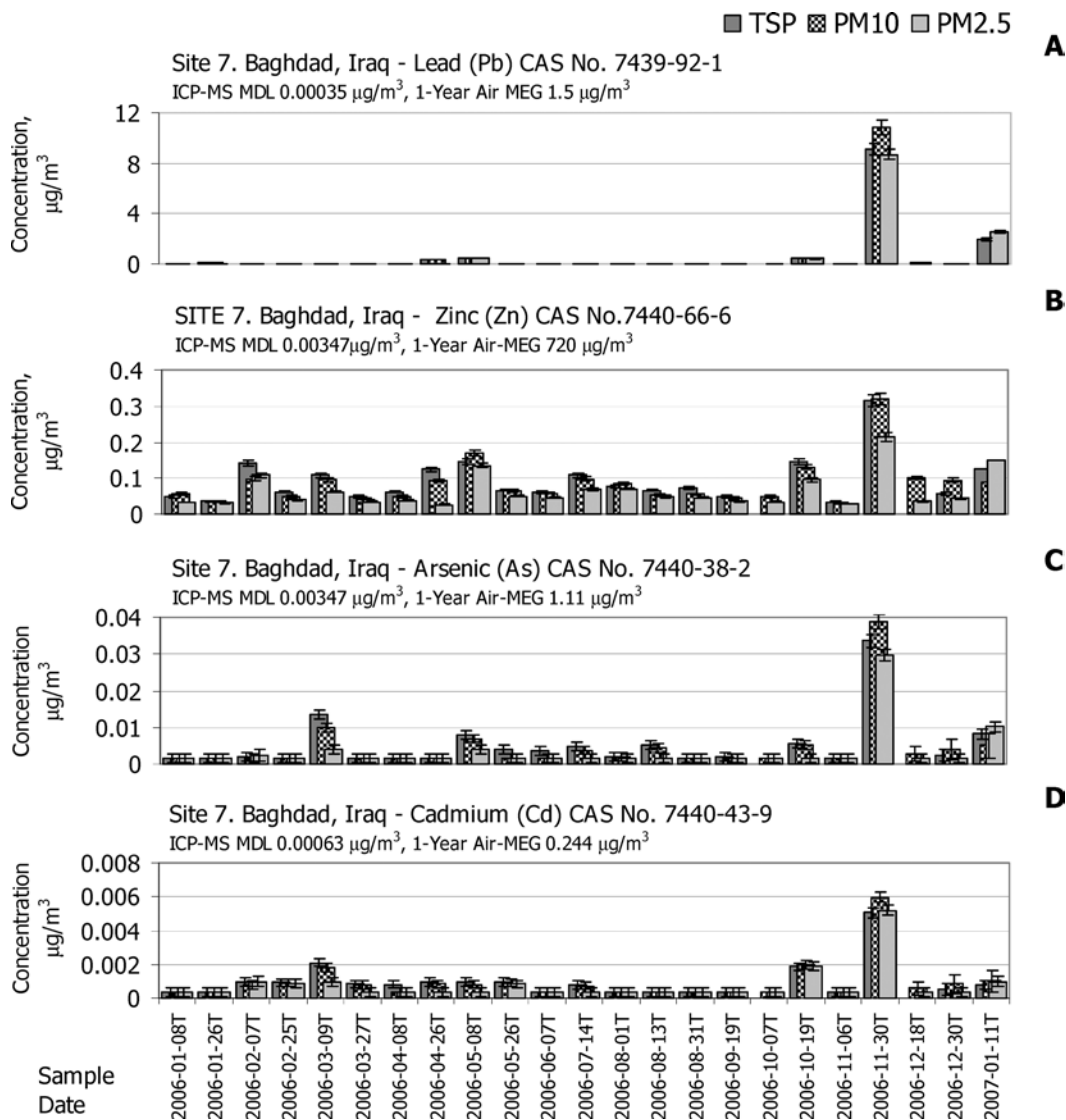


FIG. 5. Time-series plot of trace metal concentrations from Baghdad, Iraq showing corresponding elevated values for (A) lead, (B) zinc, (C) arsenic, and (D) cadmium on the 19 October 2006, 30 November 2006, and 11 January 2007 event days. These metals are concentrated in the $\text{PM}_{2.5}$ size fraction.

USACHPPM 24 h air MEG for PM_{10} ($250 \mu\text{g}/\text{m}^3$) was exceeded at 3, and for $\text{PM}_{2.5}$ ($65 \mu\text{g}/\text{m}^3$) at 7, of the 15 sites (Figure 2) by the average PM values for the sites (http://chppm-www.apgea.army.mil/documents/FACT/Particulate%20Matter_Factsheet_2008_30%20July_08_final.pdf).

The US Environmental Protection Agency's annual National Ambient Air Quality Standard for PM_{10} of $50 \mu\text{g}/\text{m}^3$ was revoked in December 2006, because of a lack of evidence linking health problems to long-term exposure to coarse particles.

Depending on the analytical method and standard or guideline applied, the chemical species aluminum, cadmium, and lead were noted as possibly exceeding maximum guideline values.

The USACHPPM 1-year interim air MEG of $3.42 \mu\text{g}/\text{m}^3$ for aluminum was on average exceeded at all 15 sites. We assume that this guideline is for aluminum metal or soluble aluminum salts. Since aluminum measured in samples from all 15 sites was identified as inert aluminum silicates (i.e. part of the crystalline mineral structure), including feldspars, micas, or clays, this guideline should not apply. The Occupational Safety and Health Administration's 8h guideline value of $5000 \mu\text{g}/\text{m}^3$ for respirable alumina (aluminum oxide), as shown in Table 4, was not exceeded.

Although the USACHPPM 1-year air MEG for cadmium of $0.244 \mu\text{g}/\text{m}^3$ was not exceeded, the WHO's guideline value of

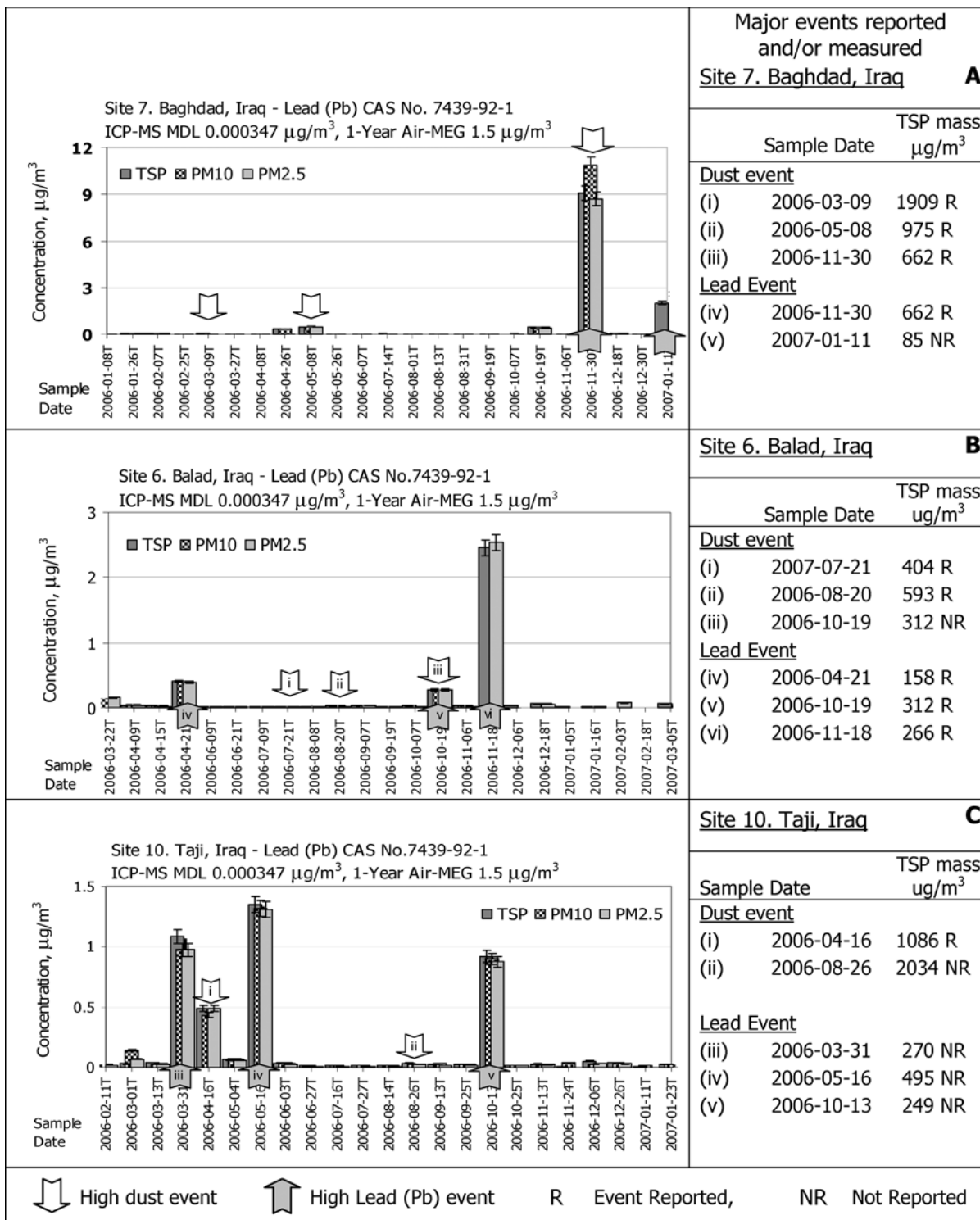


FIG. 6. Comparative time series plots of lead concentrations for (A) Baghdad, (B) Balad, and (C) Taji. The events showing elevated lead levels occur on different days for the three sites and on days for which no major regional dust storms were measured, implying local point sources for lead with fluctuating emission rates or variable meteorological conditions. High event days are listed in tables alongside the figures. Events recorded (R) or not recorded (NR) on field data sheets, together with their total TSP mass levels, are shown in the adjacent tables.

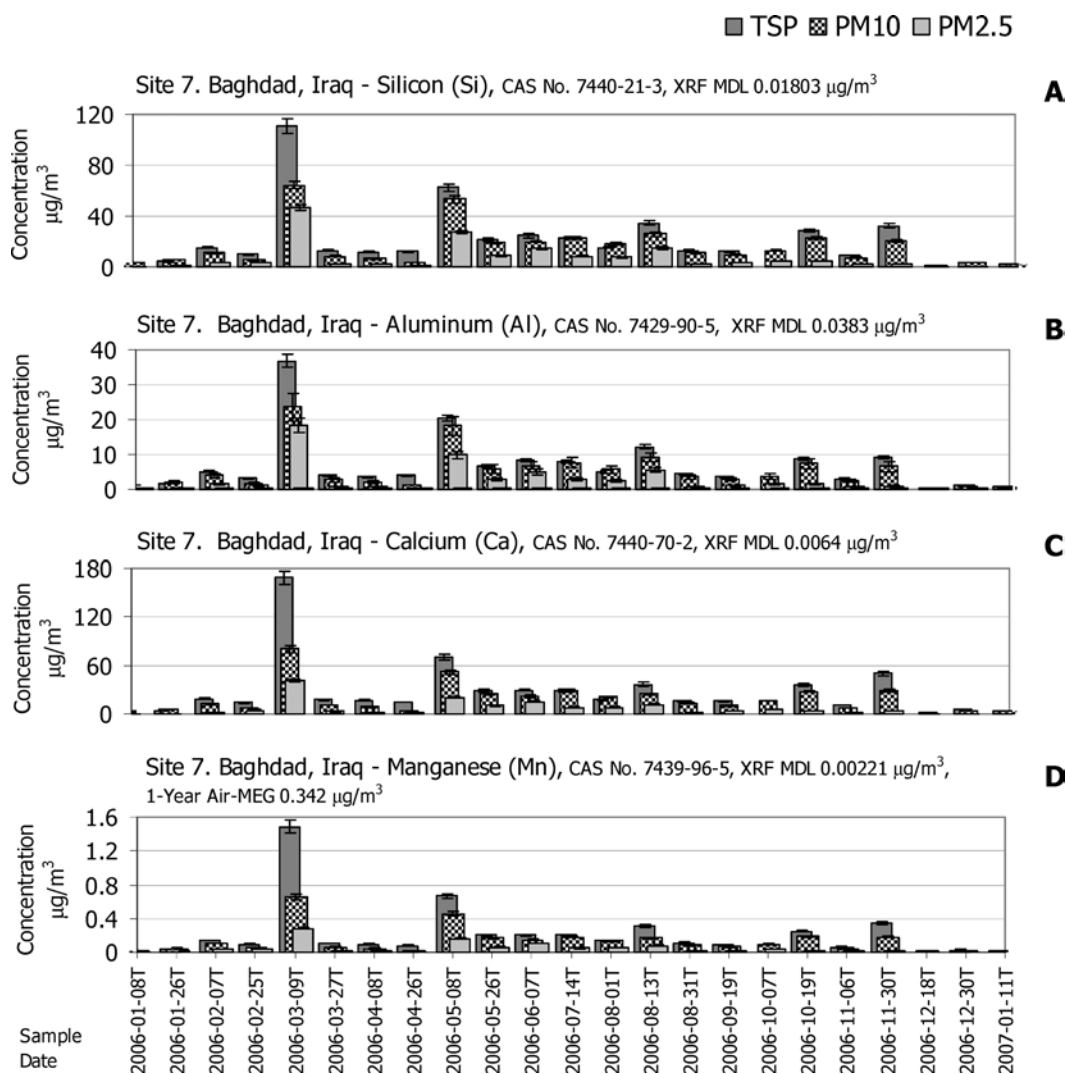


FIG. 7. Major soil-forming elements (A) silicon, (B) aluminum, (C) calcium, and (D) manganese as measured on Teflon[®] filters. Corresponding peak values represent dust blowing events on 9 March 2006, 8 May 2006, 13 August 2006, 19 October 2006, and 30 November 2006.

$0.005 \mu\text{g}/\text{m}^3$ was exceeded at all 15 sites, as measured by XRF. As measured by the more sensitive ICP-MS method, however, all 15 sites had average measured cadmium values below this WHO guideline.

Mean lead levels for all 15 sites fall within the USACHPPM 1-year MEG of $1.5 \mu\text{g}/\text{m}^3$. The average level for Baghdad, Iraq exceeds the WHO guideline of $0.5 \mu\text{g}/\text{m}^3$, as analyzed by both XRF and ICP-MS. As demonstrated below, this is largely due to a single metals emitting event on 30 November 2006, possibly from secondary lead smelters (Figures 4 and 6A).

Short-term health guidelines such as the USACHPPM 8-hour MEG, as well as National Institute of Occupational Safety and Health (NIOSH) and Occupational Safety and Health Administration standards should be considered for such short-term events.

Comparisons with Rural and Urban Sites in the US

To provide perspective on results from the 15 Middle Eastern sites, we compared these with results from five rural and five urban $\text{PM}_{2.5}$ sites in the southwestern US (Figure 3). The 10 US sites were selected because of their proximity to military bases in drier regions of the US. Average particulate matter and chemical values were calculated for the period 2002–2006.

The five rural sites are at Dome Land National Wildlife Area, Joshua Tree National Park, Bosque del Apache National Wildlife Refuge, Salt Creek National Wildlife Refuge, and San Andres National Wildlife Refuge, which form part of the Interagency Monitoring of Protected Visual Environments (IMPROVE) air-quality-monitoring network (<http://vista.cira.colostate.edu/improve/>).

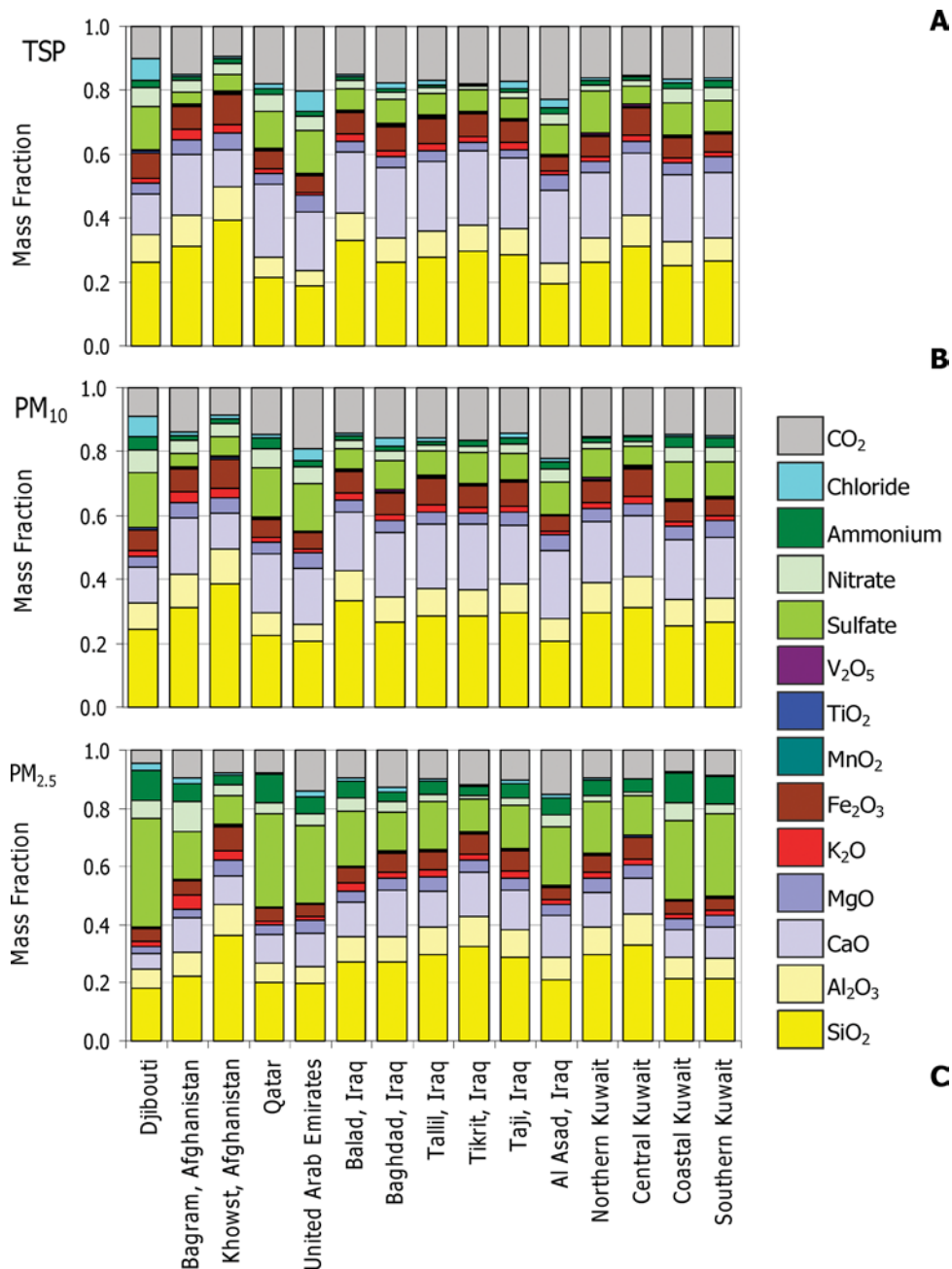


FIG. 8. Annual mean major chemistry for (A) TSP, (B) PM_{10} , and (C) $PM_{2.5}$. Concentrations are expressed as mass fractions of oxides, sulfate (in gypsum), chloride (in salt), nitrate, and ammonium.

The five urban sites are in Las Vegas (Nevada), Los Angeles (California), Tucson (Arizona), Albuquerque (New Mexico), and El Paso (Texas) and form part of the US Environmental Protection Agency's Chemical Speciation Network (CSN) monitoring program (<http://www.epa.gov/ttn/airs/airsaqs/detaildata/downloaddata.htm>).

Average $PM_{2.5}$ mass and chemical concentration levels from the deployment sites are—except for a few species such as nitrate, sodium, and rubidium—greater than chemical abundances

in $PM_{2.5}$ samples measured at rural IMPROVE and urban CSN sites in the southwestern US.

Trace Metals

Annual mean ICP-MS trace-metal analysis results of 12 chemical species were compiled per size-cut (TSP , PM_{10} , $PM_{2.5}$) and sampling site (Figure 4). Lead is the most abundant trace species found in Baghdad aerosol and also contributes substantially to measured trace metals at Taji and Balad. It is of note that,

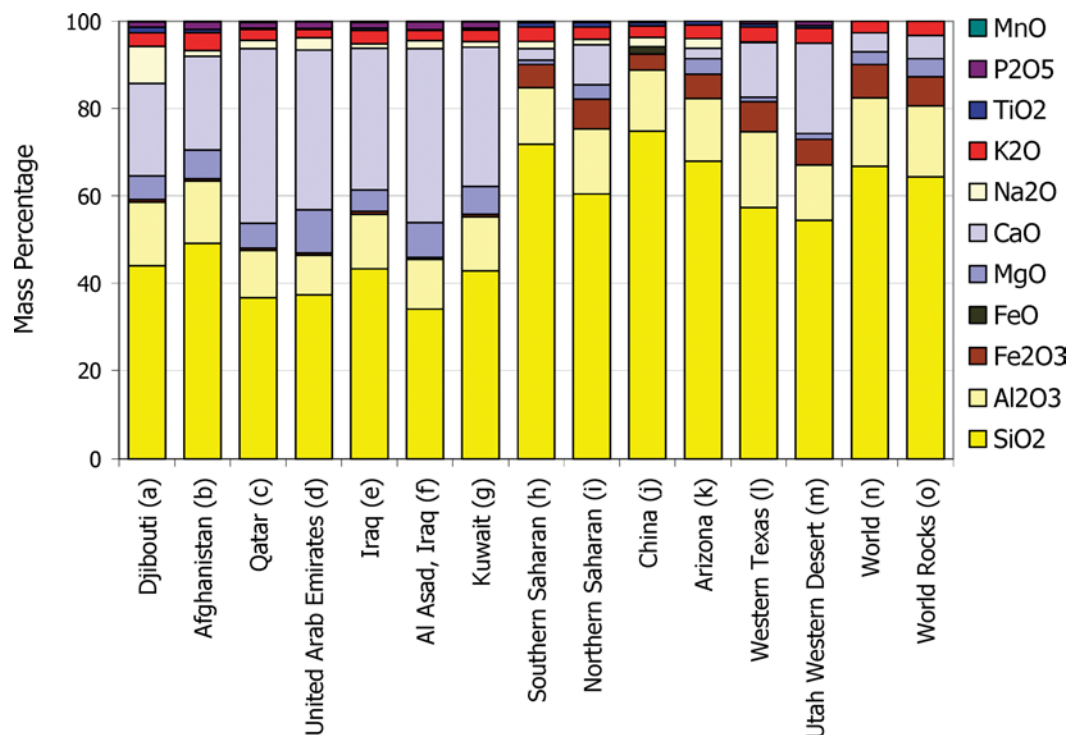


FIG. 9. Comparison of dust samples from the Middle East, Sahara, China, US, world average dust, and world rocks. In the case of the EPMSF samples, mean TSP results are shown: (a) Djibouti; (b) Bagram and Khowst in Afghanistan; (c) Qatar; (d) the UAE; (e) Balad, Baghdad, Tallil, Tikrit, and Taji in Iraq; (f) Al Asad in Iraq; (g) Northern, Central, Coastal, and Southern Kuwait; (h) average Southern Sahara (Goudie, 2006); (i) average Northern Sahara (Goudie, 2006); (j) average China (Goudie, 2006); (k) Arizona (Goudie, 2006); (l) Western Texas (Labban et al., 2004); (m) Utah Western Desert (Labban et al., 2004); (n) average world dust (Goudie, 2006); and (o) average world crustal rocks (Clarke, 1916).

TABLE 5

For ambient samples, the number of Nuclepore[®] filters analyzed by computer-controlled scanning electron microscopy (CCSEM) for each sampled size fraction

Site No.	Site locality	Site ID	TSP	PM ₁₀	PM _{2.5}	Total
1	Djibouti	DJI_LEM	2	9	4	15
2	Bagram, Afghanistan	AFG_BAG	2	9	6	17
3	Khowst, Afghanistan	AFG_SAL	1	10	5	16
4	Qatar	QAT_UDE	1	10	5	16
5	United Arab Emirates	UAE_DHA	3	8	7	18
6	Balad, Iraq	IRQ_ANA	1	10	5	16
7	Baghdad, Iraq	IRQ_VIC	2	7	7	16
8	Tallil, Iraq	IRQ_ADD	2	9	7	18
9	Tikrit, Iraq	IRQ_SPE	2	3	4	9
10	Taji, Iraq	IRQ_TAJ	2	8	7	17
11	Al Asad, Iraq	IRQ_ALA	2	9	9	20
12	Northern Kuwait	KUW_BUE	1	8	7	16
13	Central Kuwait	KUW_AAS	1	8	5	14
14	Coastal Kuwait	KWT_SHU	1	10	5	16
15	Southern Kuwait	KUW_ARI	2	9	8	19
	Total		25	127	91	243

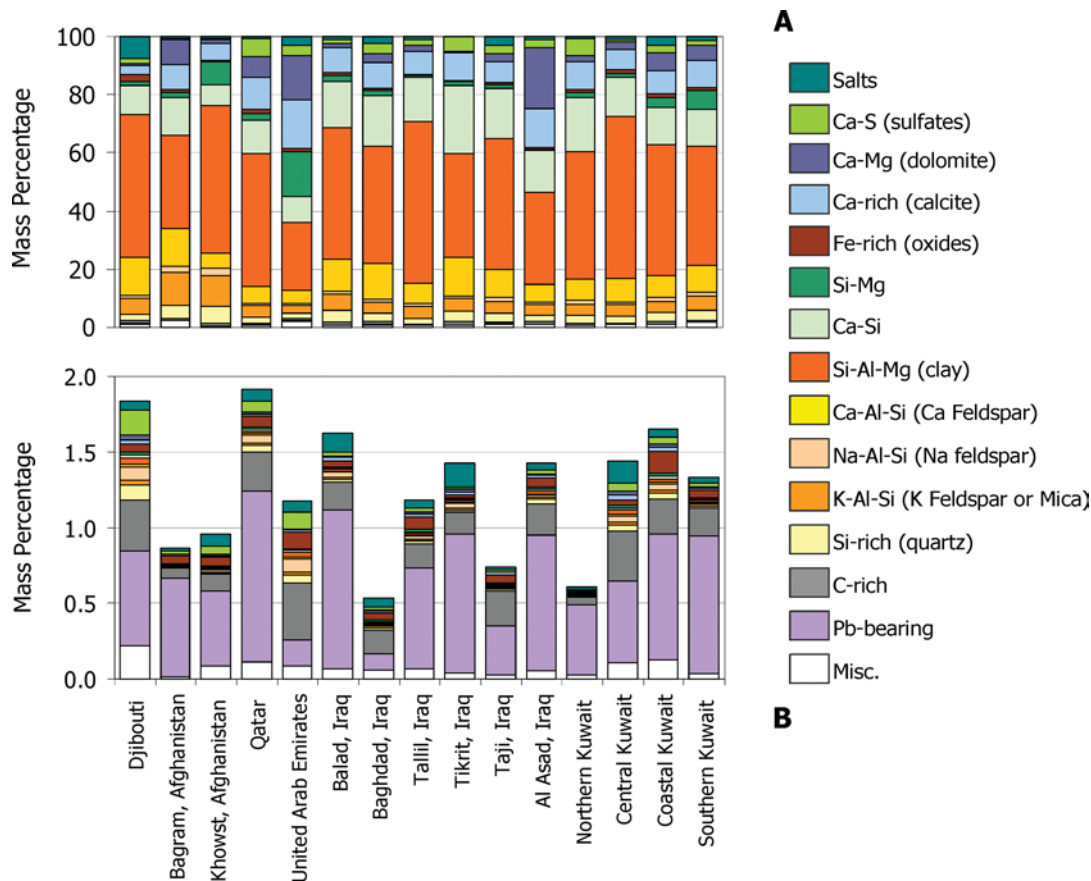


FIG. 10. Composite of all CCSEM PM_{10} results measured on Nuclepore[®] filters, grouped by site. All size fractions, from $0.5 \mu\text{m}$ to $10 \mu\text{m}$ diameter particles, are shown in (A), while the $0.5\text{--}1.0 \mu\text{m}$ diameter (fine fraction) subset is shown in (B), demonstrating that lead (Pb) is concentrated in this fine fraction.

for all sites, the lead concentrations (in $\mu\text{g}/\text{m}^3$) are nearly identical for the three size fractions (TSP, PM_{10} , $PM_{2.5}$). Since PM_{10} is contained in TSP and $PM_{2.5}$ in PM_{10} , this implies that most, if not all, the lead occurs in the $PM_{2.5}$ size fraction. Most combustion products (elemental carbon and particulate organic compounds) also occur in the fine ($PM_{2.5}$) and ultra-fine fractions, and some lead may be a component of combustion products for these locations. Fine lead and zinc, together with other associated metals, also are generated from condensed fumes emitted by metallurgical processes such as lead-zinc smelters or backyard electronic circuit board smelting operations (Carroll & Essik, 2008). Lead also occurs as an additive in leaded gasoline and is emitted with gasoline vehicle emissions.

A major lead emitting event, far exceeding the USACHPPM 1-year air MEG value of $1.5 \mu\text{g}/\text{m}^3$, was recorded at the Baghdad site on 30 November 2006, with a smaller spike on 11 January 2007, and a few other days (Figure 5A). Similar elevated concentration levels also were recorded for zinc (Figure 5B), arsenic (Figure 5C), and cadmium (Figure 5D) on the same days. This implies that these (and antimony) trace metals were emitted by the same or a collocated source.

Very low concentration levels of arsenic and cadmium were measured in TSP and PM_{10} , and in lower concentrations in $PM_{2.5}$, on 9 March 2006 and 8 May 2006—most likely associated with dust events on those 2 days. Similar associations among lead, arsenic, cadmium, and antimony were measured at Balad and Taji, pointing to a similar source type, such as secondary lead battery and electronic-circuit-board smelters affecting all three sites. The relationship between known dust events and elevated lead emissions for the three sites at Baghdad, Taji, and Balad is shown in Figure 6. The table alongside each time series plot shows the recorded high-dust days and corresponding measured TSP levels. There is little concordance between the high dust and high lead days, pointing to two distinct but different sources—one for geological dust and the other for trace metals (lead, arsenic, cadmium, antimony, zinc). Lead spikes occur on different days for each of the three monitoring sites, indicating different wind directions for point sources in relation to the monitoring sites, as well as variable meteorological conditions. The presence of individual particles of zinc and lead as well as lead in vehicle emissions, from the Balad–Baghdad–Taji region were confirmed by SEM–EDS (Figures 12 and 13).

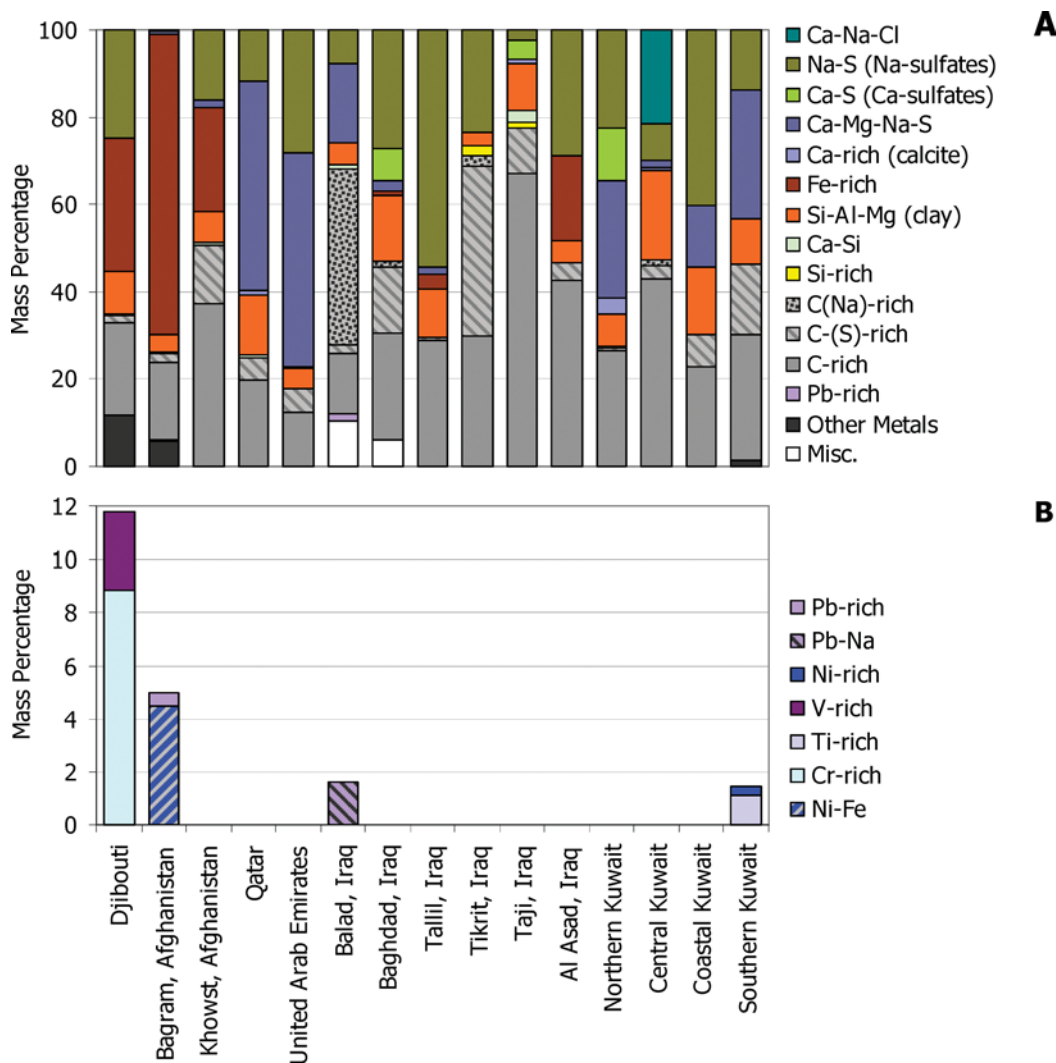


FIG. 11. SEM and CCSEM results of ultrafines ($<0.5 \mu\text{m}$ diameter) measured on 15 $\text{PM}_{2.5}$ samples collected on Nuclepore[®] filters. Compositions of 100 particles analyzed for all species are shown in (A), while individual minor and trace metals are shown on an expanded scale in (B).

A further trace element of interest is manganese, which was highest at Tikrit (Table 4). The highest manganese concentrations occurred in TSP and PM_{10} , and the lowest concentrations in the $\text{PM}_{2.5}$ fraction. For all 15 sites, manganese is associated with the coarse fraction of dust corresponding to days of high particulate matter concentrations and also to recorded dust events (Figure 7D).

Major Chemical Species

Elevated levels of major chemical species occur during dust events at all 15 sites. In the case of Baghdad, major dust events were recorded on 9 March 2006, 8 May 2006, 13 August 2006, 19 October 2006, and 30 November 2006. This is reflected by the time-series plots for silicon, aluminum, calcium, and man-

gane (Figure 7), which are similar for iron, magnesium, potassium, and sodium. The large mass differences between the TSP and PM_{10} , as well as PM_{10} and $\text{PM}_{2.5}$, soil-forming components show that these chemical species are largely in coarse dust fractions. As previously shown (Table 3), the coarse minerals contain the major chemical species; the proportion of mineral dust in the $\text{PM}_{2.5}$ fraction is small (on average <38).

Total particulate matter distribution (Figure 2) is reflected in the total major element distribution patterns—with Tikrit, Tallil, and Central Kuwait having the highest average total major element concentrations. The mass fractions of major chemical species are graphically presented as oxides, nitrate, sulfate, ammonium, and chloride (Figure 8). Although there are differences among some sites, there is consistency among the three size

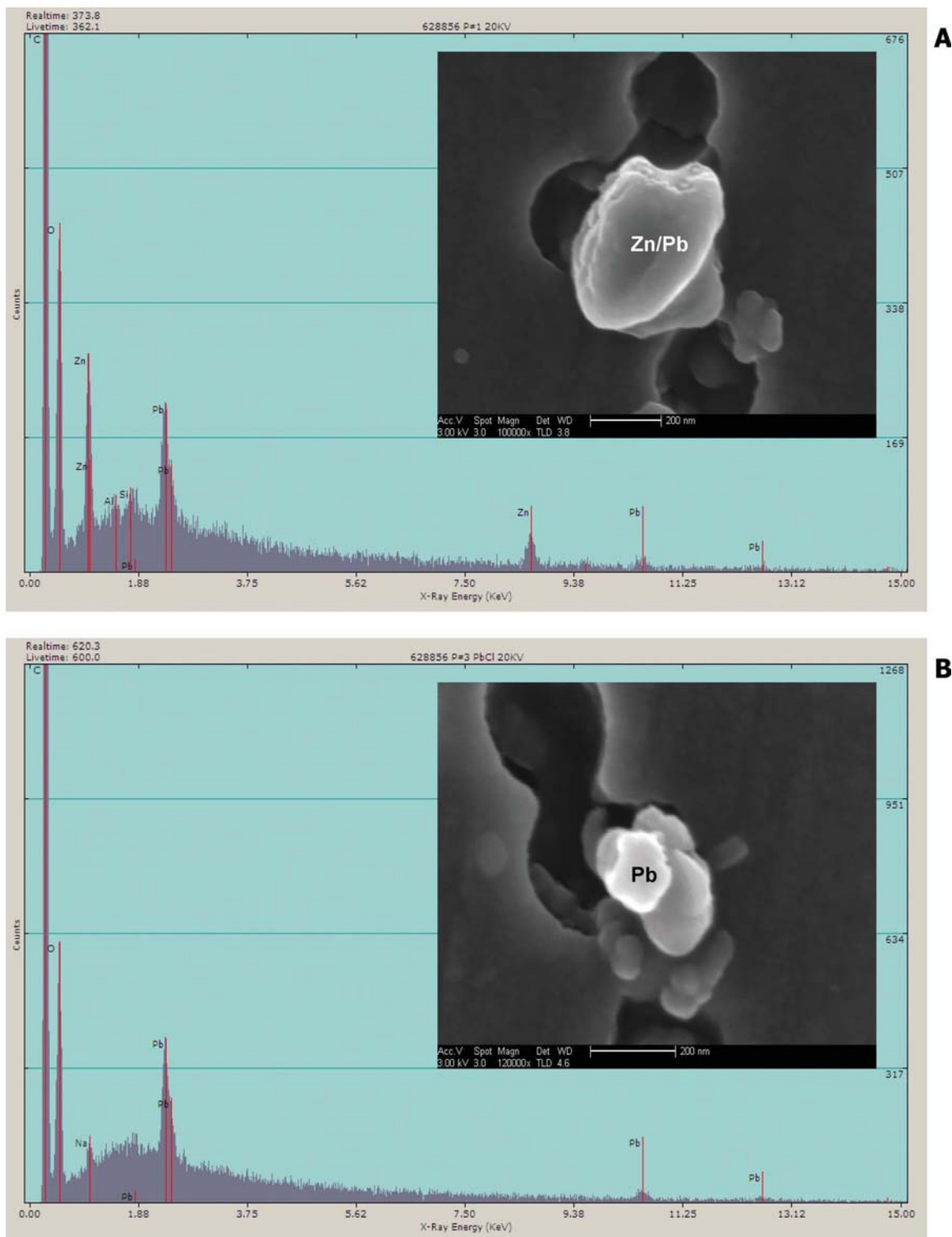


FIG. 12. Secondary electron images and EDS spectra of two particles on a Nuclepore[®] filter sampled in Balad, Iraq: (A) zinc/lead (Zn/Pb) particle with carbon, possibly from a lead and dry cell battery smelting facility; and (B) lead (Pb) particle from lead smelting. Dark circles in the field are approximately 0.4 μm pores in the Nuclepore[®] membrane filters.

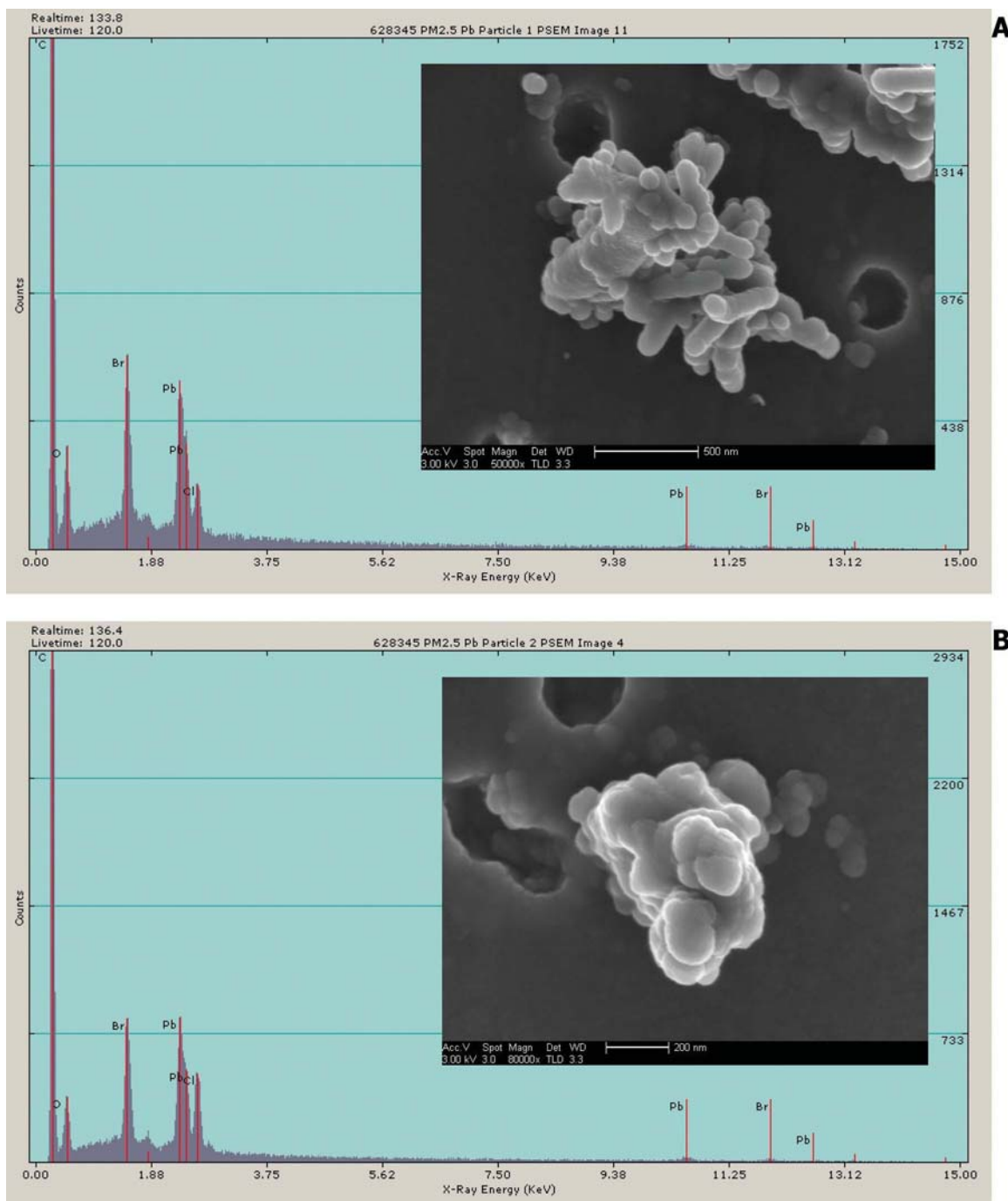


FIG. 13. Secondary electron images and EDS spectra of two particles on a Nuclepore[®] filter sampled in Balad, Iraq. Both (A) and (B) are sections of carbon chains containing high concentrations of lead (Pb), bromine, and chlorine often associated with emissions from leaded gasoline vehicles.

fractions: TSP and PM₁₀ are similar for all 15 sites. Mass fractions of SiO₂ are smallest in PM_{2.5}, because this oxide is largely contained in hard and coarse mineral quartz. The SiO₂ content is the highest at Khowst in Afghanistan for all size fractions; this finding can be ascribed to a high percentage of SiO₂-rich silt in

local dust. Similarly, CaO and CO₂, which are both contained in the carbonate mineral calcite, have slightly higher mass fractions in TSP and PM₁₀.

Chloride from sea salt was found in TSP and PM₁₀ at Djibouti, a site on the Gulf of Aden. Sulfate, partly as secondary

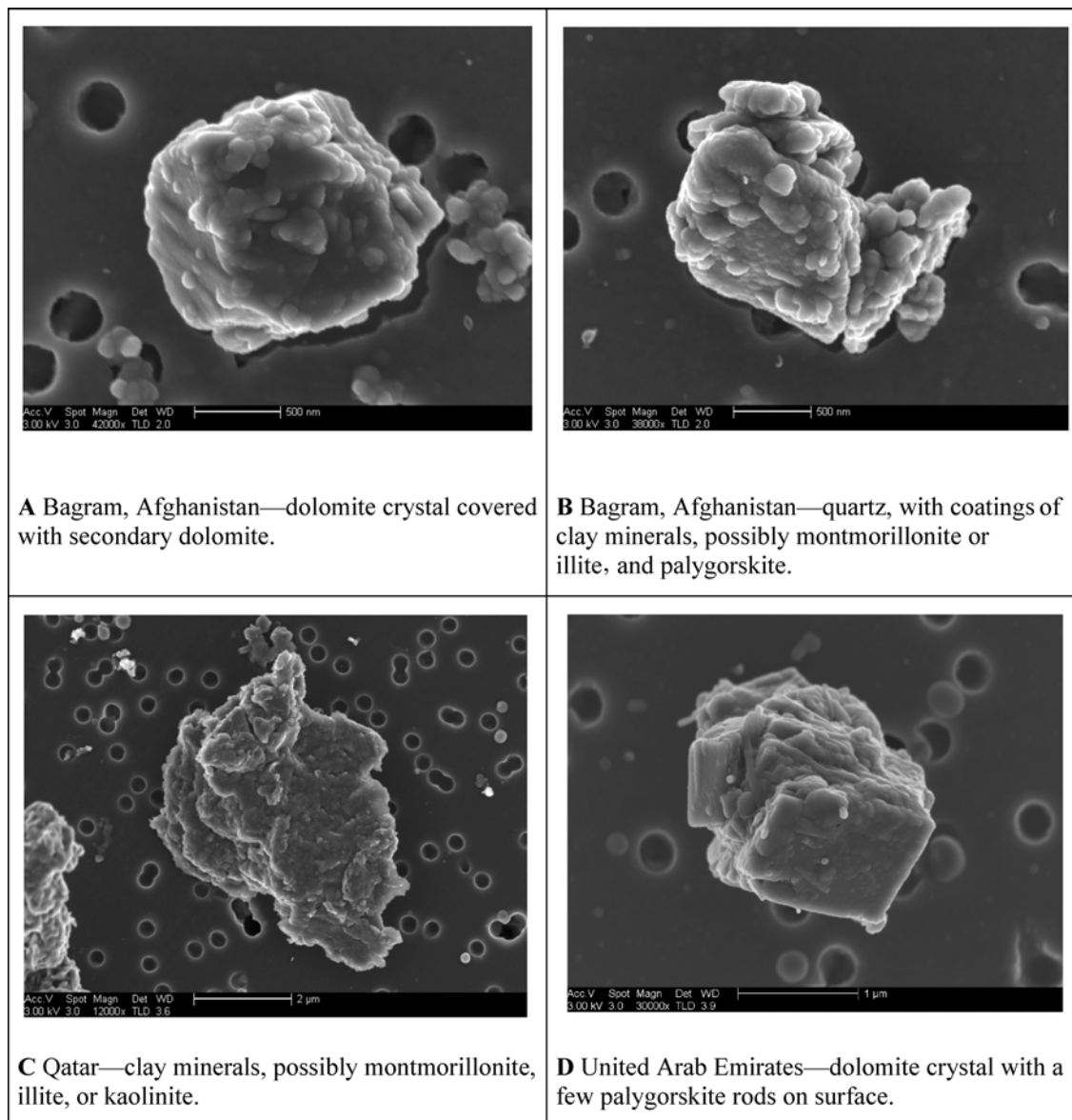


FIG. 14. Secondary electron images from Bagram (A and B), Qatar (C), and United Arab Emirates (D) samples. Dark circles in the field are approximately $0.4 \mu\text{m}$ pores in the Nuclepore[®] membrane filters.

ammonium sulfate and also as gypsum, is concentrated in the $\text{PM}_{2.5}$ size fraction. High concentrations of sulfate were found in $\text{PM}_{2.5}$ at Djibouti, Qatar, UAE as well as Coastal and Southern Kuwait. Sulfate as secondary ammonium sulfate was in all likelihood from sulfur dioxide emissions from petrochemical and other industries in the Middle East. Compared to the other sites, UAE and Al Asad samples had slightly higher CaO, MgO, and CO_2 contents representing contributions from calcite and dolomite soils in these two regions (Engelbrecht et al., in press).

In general, analyzed dust from these 15 Middle East sites are not considered to be out of the ordinary. A comparison of TSP filter chemistry from this program with dust from various

parts of the southwestern US, Sahara, and China is given in Figure 9. Most dust samples contain mixtures of silicate minerals, carbonates, oxides, sulfates, and salts, in various proportions, as reflected by their chemistry. Differences lie in the relative proportions of these minerals and subsequent chemical components. Compared with the Sahara, China, US, and world dusts, Middle East samples had lower proportions of SiO_2 and higher proportions of CaO and MgO. The last two components are contained in the carbonate minerals calcite and dolomite and were found in higher concentrations at the UAE and Al Asad sites. Fe_2O_3 and MnO occur as various iron–manganese minerals, found in greater concentrations in the Sahara, China and US

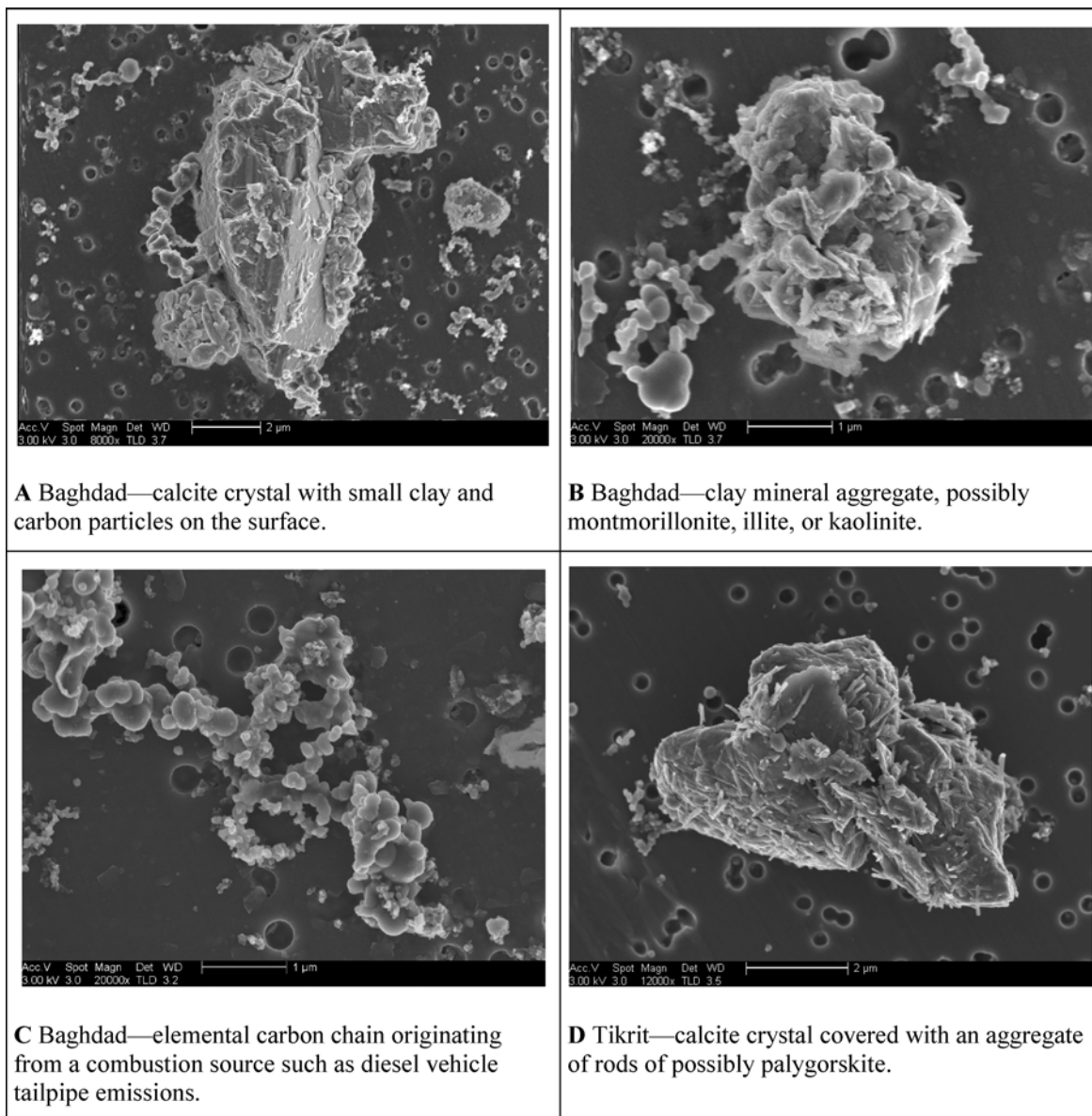


FIG. 15. Secondary electron images from Baghdad (A–C) and Tikrit (D). Dark circles in the field are approximately $0.4 \mu\text{m}$ pores in the Nuclepore[®] membrane filters.

when compared with the Middle East sample sets. Al_2O_3 , a major constituent of clay minerals and other silicates, was found to be similar for most dusts. Sodium generally occurs as salt from evaporated sea water as well as saline desert areas.

Electron Microscopy

SEM provided chemical and morphological information about individual particles collected on Nuclepore[®] filters at each of the 15 sites. Chemical compositions of the individual particles were similar to chemical composition results from the Teflon[®] and quartz fiber filter samples collected in the ambient atmosphere at these sites. CCSEM provided chemical and mor-

phological analyses of approximately 1,000 particles per filter measured on a total of 243 Nuclepore[®] filters (Table 5).

Figure 10A presents results of 3–10 compounded PM_{10} Nuclepore[®] filters from each of the 15 sampling sites. Particles were classed into chemical ‘bins’, some of which were interpreted as minerals, based on XRD measurements of $<38 \mu\text{m}$ sieved soil samples (Engelbrecht et al., in press). In this fashion, we interpreted Ca-Mg particles as dolomite, Ca-rich as calcite, Si-Al-Mg rich as clay, Si-rich as quartz, and so on. The ‘bin’ with the highest mass fraction at all 15 sites is Si-Al-Mg (clay), varying from 27% for UAE to 59% for Tallil. Except for UAE and Al Asad, which have higher concentrations

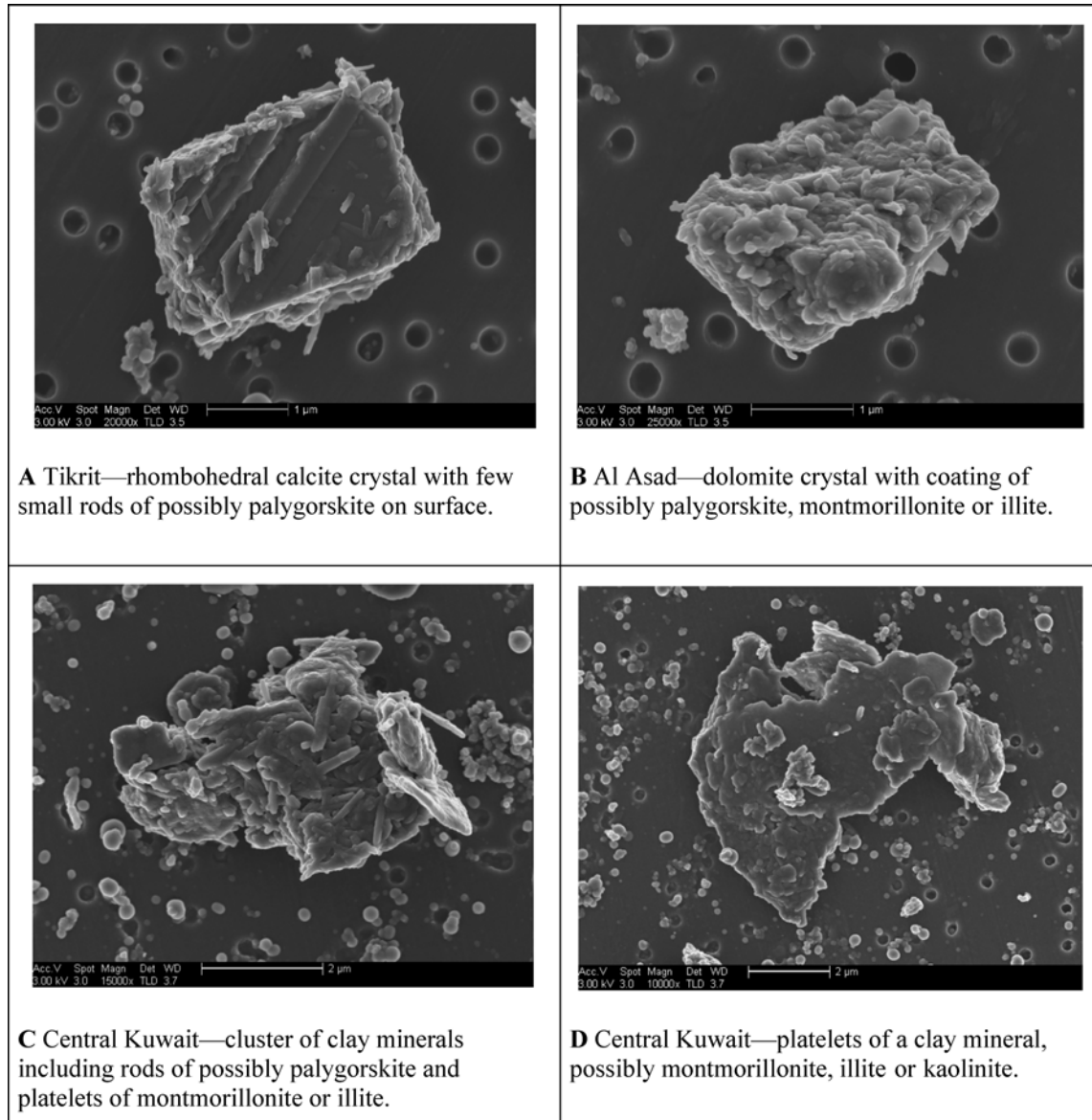


FIG. 16. Secondary electron images from Tikrit (A), Al Asad (B), and central Kuwait (C and D). Dark circles in the field are approximately $0.4 \mu\text{m}$ pores in the Nuclepore[®] membrane filters.

of carbonate (calcite and dolomite respectively), and the UAE, which has a higher Si-Mg particle content, there is similarity among the sites. What is evident from these CCSEM results is the low percentage of Si-rich (quartz) particles, considering substantial amounts of quartz were measured by XRD (Engelbrecht et al., in press) and supported by XRF results (Figure 8). Direct comparisons cannot be made in all instances, since XRD was performed on the $<38 \mu\text{m}$ sieved fraction and chemical analysis on filter samples. In general, the proportion of quartz decreases toward the finer dust fractions, with an increase in the softer clay minerals. Our interpretation of the CCSEM measurements is that quartz and other silicate minerals, as well as dolomite,

and calcite particles to a limited degree, are often coated by clay minerals such as palygorskite, montmorillonite, and illite. The CCSEM provides good measurements of surface coatings on quartz and other mineral grains, but the coated mineral grains result in underestimation of the total particle mineralogy using this analytical technique.

Figure 10B presents the $0.5\text{--}1.0 \mu\text{m}$ subset from the Figure 10A data set. As with trace metal results (Figure 4), this demonstrates that lead-bearing aerosol particles are concentrated in the finer fraction on Nuclepore[®] filters.

Summary plots of the ultrafine fractions, as measured by SEM, are graphically presented in Figure 11. A total of 100

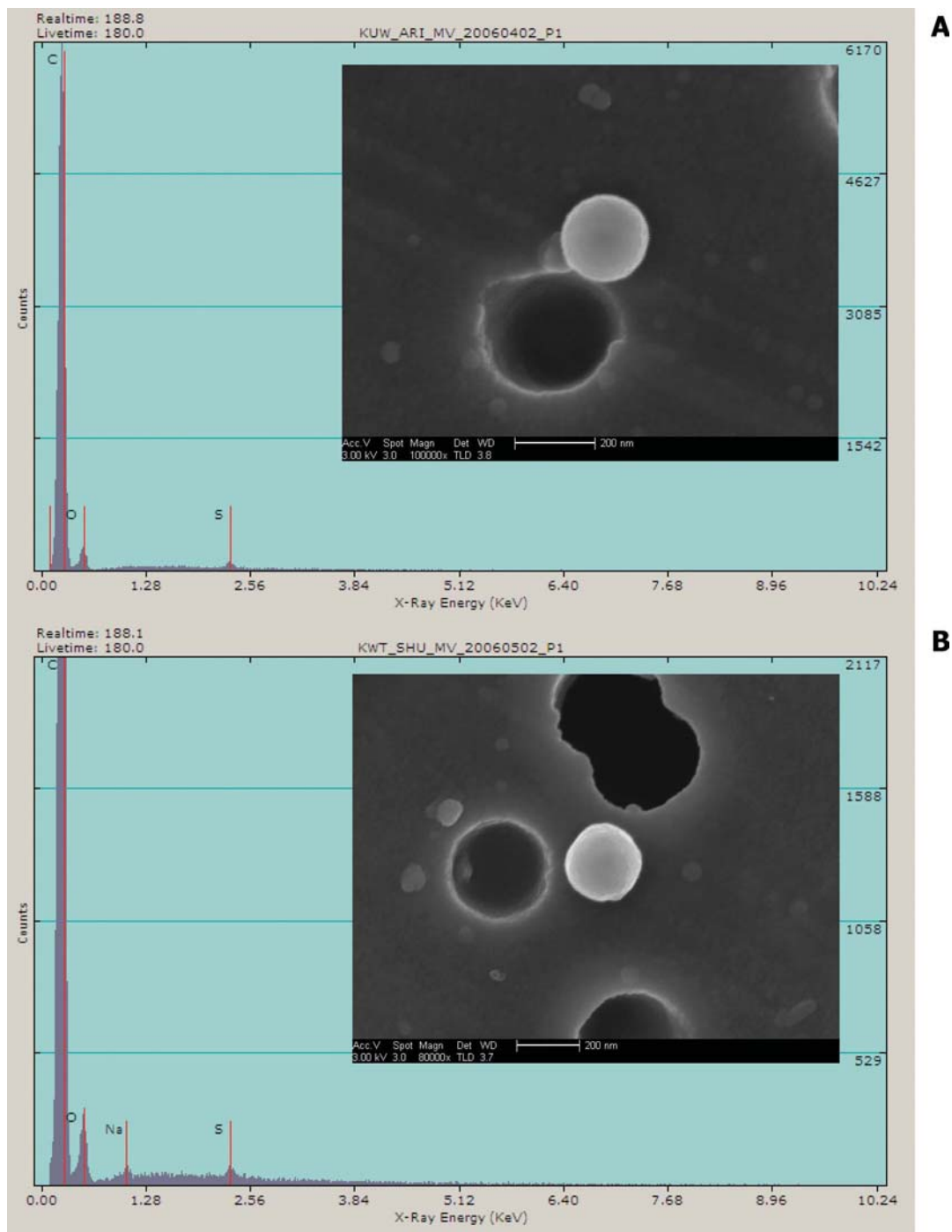


FIG. 17. Secondary electron images and EDS spectra of two spherical ultrafine (approx. 0.2 μm diameter) particles on Nuclepore® filters: (A) carbon particle with sulfur from Southern Kuwait and (B) carbon particle with sodium and sulfur from Coastal Kuwait. Both particles may be from combustion of sulfur-rich oil, including diesel fuel. Dark circles in the field are approximately 0.4 μm pores in the Nuclepore® membrane filters.

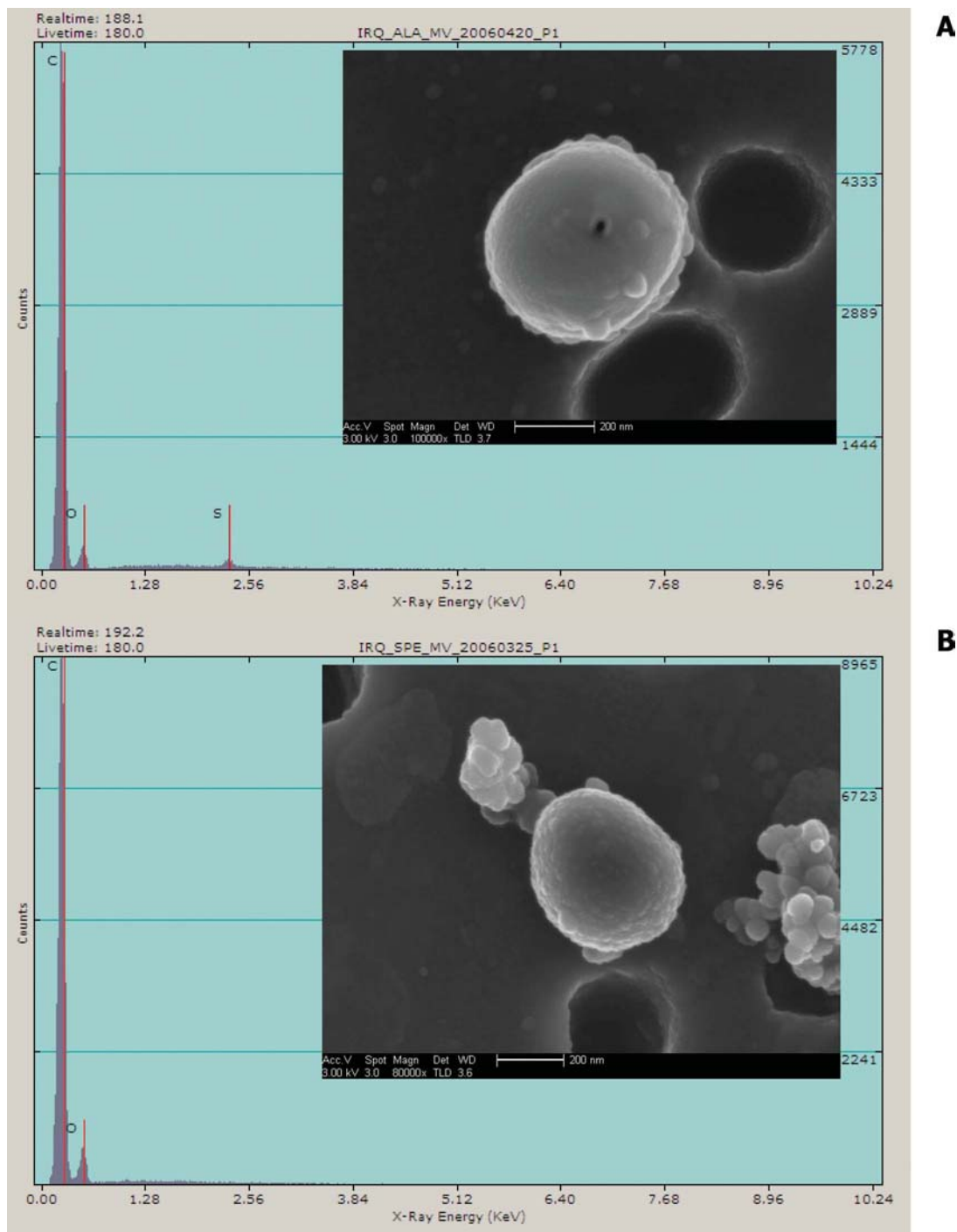


FIG. 18. Secondary Electron Images and EDS spectra of two spheroids of ultrafine (approx. $0.5 \mu\text{m}$ diameter) particles on Nuclepore[®] filters: (A) carbon particle with sulfur from Al Asad and (B) carbon particle from Tikrit in Iraq. Both particles may be from the combustion of oil, including diesel fuel. Dark circles in the field are approximately $0.4 \mu\text{m}$ pores in the Nuclepore[®] membrane filters.

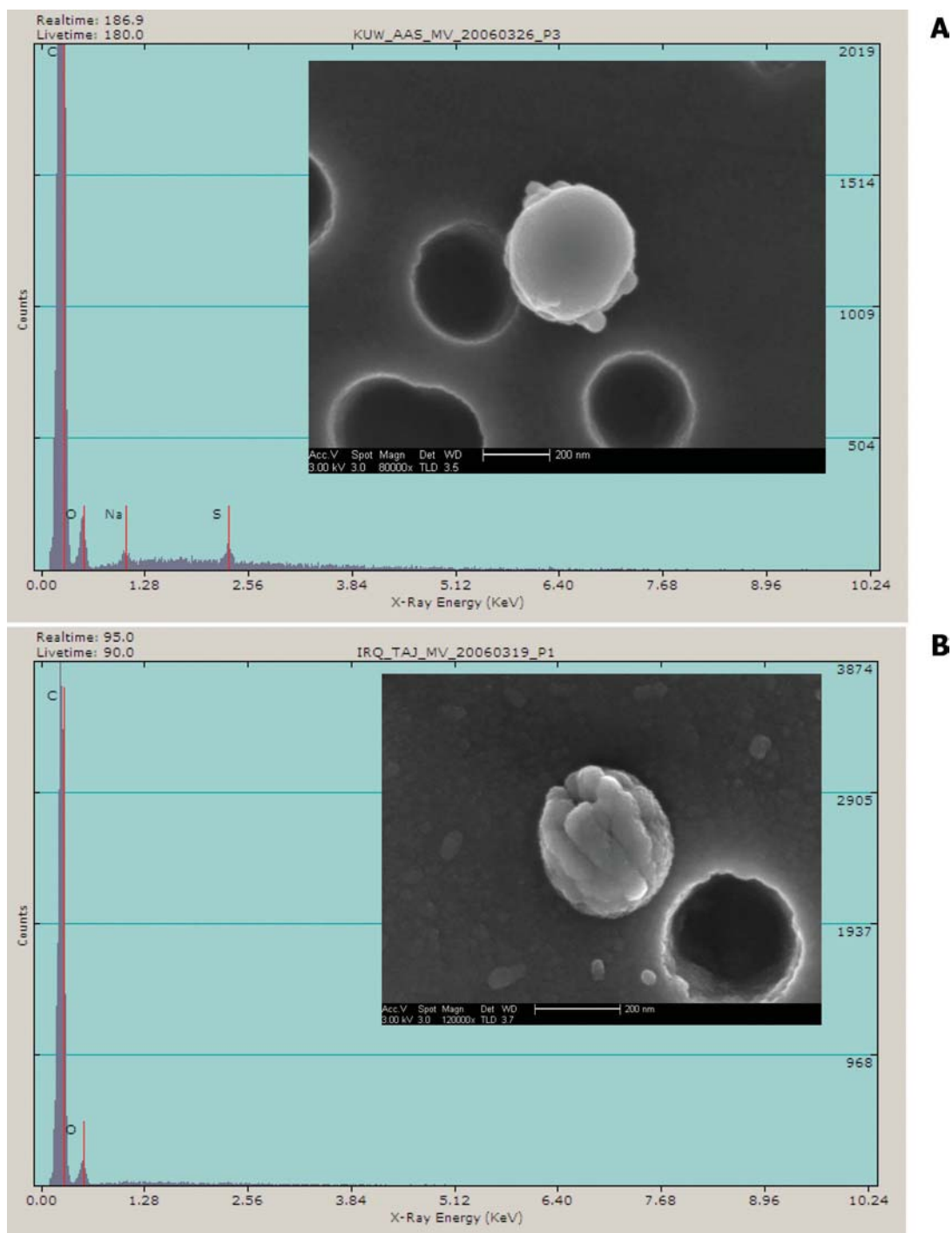


FIG. 19. Secondary electron images and EDS spectra of two spheroids of ultrafine (approx. $0.4 \mu\text{m}$ diameter) particles on Nuclepore[®] filters: (A) carbon-sodium-sulfur particle from central Kuwait, (B) carbon particle composed of smaller carbon particles from Taji, Iraq. Both particles may be from oil-combustion processes. Dark circles in the field are approximately $0.4 \mu\text{m}$ pores in the Nuclepore[®] membrane filters.

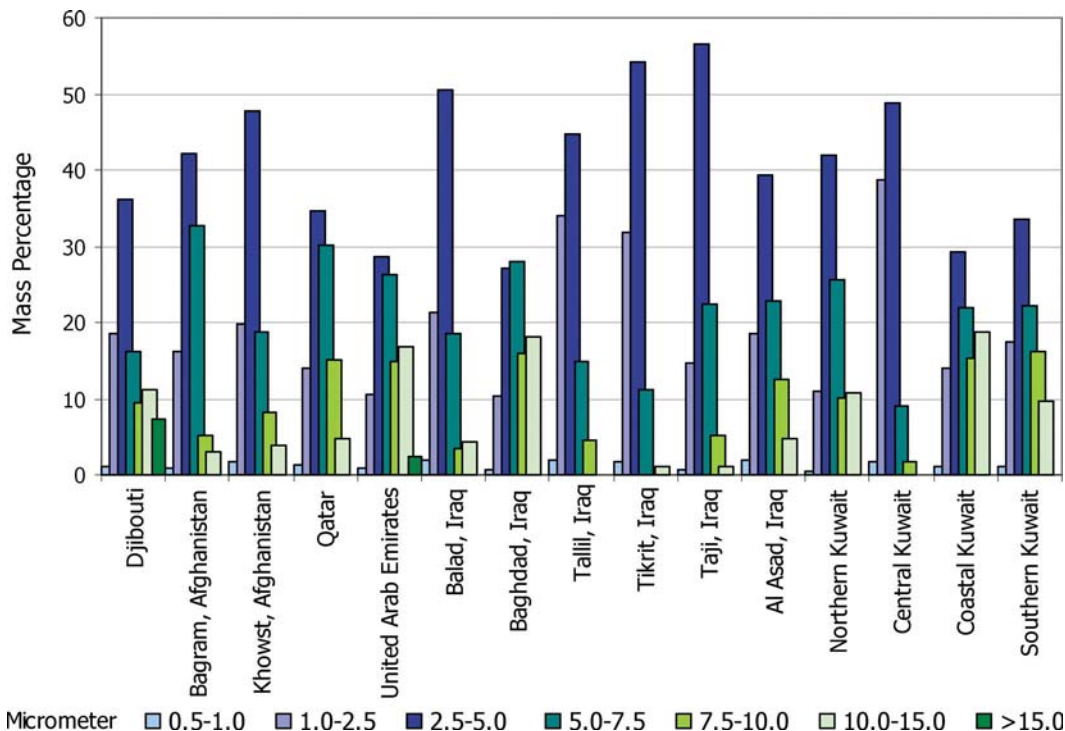


FIG. 20. Particle-size distributions by mass percentage, as measured by CCSEM, of TSP samples collected on Nuclepore[®] filters.

particles $<0.5 \mu\text{m}$ in diameter were analyzed on Nuclepore[®] membrane filters: one $\text{PM}_{2.5}$ filter from each of the 15 sites. Because of the small particle sizes, 50 particles $<0.2 \mu\text{m}$ from each filter were manually analyzed by SEM, and another 50 particles $0.2\text{--}0.5 \mu\text{m}$ in diameter were analyzed by interactive CCSEM. The purpose was to establish if trace metals or particles of concern are concentrated in this size fraction. From particle-size distribution patterns (Figure 20), total mass in the ultrafine size fraction was estimated to be far less than 1% of total mass on the filters.

Chemistry and morphology of the ultrafines were found to differ substantially from those of the coarser fractions. The former contains far less geological components (e.g. silicon, aluminum, iron, manganese, calcium, or magnesium) than the coarser fractions. Ultrafines very often contain spheroidal particles of carbon, together with sulfur, sodium, and chlorine (Figures 17–19) and, in a few instances, lead, bromine, and chlorine (Figure 13). The origin of the spheroids is uncertain, but it can be assumed from their carbon and sulfur content that many of these are from various oil, gasoline, and natural-gas combustion processes, including motor-vehicle emissions. Chromium-rich and vanadium-rich particles typical of igneous rocks from the Rift Valley region were analyzed in ultrafines from Djibouti (Figure 11B). Trace amounts of nickel from Bagram, as well as titanium and nickel from Southern Kuwait, may be of geological origin. Lead measured in the Balad sample is likely to be from lead smelters and gasoline vehicle emissions.

Lead on the Bagram filter is probably from gasoline vehicle emissions.

Transmission electron microscope measurements for airborne asbestos were performed on one Nuclepore[®] filter from each site. No asbestos fibers were found using this method (Yamate et al., 1984).

Figures 12–19 are high-resolution secondary electron images of mineral grains from selected sampling sites. These images show a variety of crystal forms, including dolomite and calcite, as well as aggregates and coatings of clay minerals. Although detailed clay mineral analysis was not performed on these samples, several findings regarding the clays of the Middle East (Kahlaf et al., 1985; Cagatay, 1990; Al-Jaboury, 2006), as well as our CCSEM and secondary electron images, are evidence for Mg-Al-Si particles being a clay phase. We interpret rods and fibers as palygorskite (Figures 15D and 16C) and the platelets as montmorillonite or montmorillite mixed layers or kaolinite (Figures 14C, 15B, and 16D).

A particle size distribution for each of the 15 sites was compiled from the composite (1–3 filters) TSP Nuclepore[®] samples. All sites show a positive skewed distribution, and all except Baghdad have a distinct maximum in the $2.5\text{--}5.0 \mu\text{m}$ size range (Figure 20, Table 6). Distributions from the Djibouti, the UAE, Balad, Baghdad, and northern and coastal Kuwait samples have a slightly bimodal concentration, with a minor peak in the $10\text{--}15 \mu\text{m}$ size range. We ascribe these to wind-blown dust events producing large particles.

TABLE 6

Particle-size distributions by mass percentage, as measured by computer-controlled scanning electron microscopy (CCSEM) on Nuclepore[®] filters.

Bin Size Site No.	Site locality Site ID	0.5–1 μm %	1–2.5 μm %	2.5–5 μm %	5–7.5 μm %	7.5–10 μm %	10–15 μm %	>15 μm %
1	Djibouti DJL_LEM	1.2	18.6	36.2	16.1	9.5	11.2	7.3
2	Bagram, Afghanistan AFG_BAG	0.9	16.1	42.1	32.6	5.2	3.1	0.0
3	Khowst, Afghanistan AFG_SAL	1.8	19.8	47.8	18.6	8.1	3.9	0.0
4	Qatar QAT_UDE	1.3	14.0	34.7	30.1	15.2	4.7	0.0
5	United Arab Emirates UAE_DHA	0.8	10.4	28.6	26.2	14.8	16.7	2.4
6	Balad, Iraq IRQ_ANA	1.9	21.2	50.5	18.6	3.5	4.4	0.0
7	Baghdad, Iraq IRQ_VIC	0.6	10.3	27.0	28.0	15.9	18.1	0.0
8	Tallil, Iraq IRQ_ADD	1.9	34.1	44.7	14.8	4.5	0.0	0.0
9	Tikrit, Iraq IRQ_SPE	1.7	31.8	54.2	11.2	0.0	1.1	0.0
10	Taji, Iraq IRQ_TAJ	0.6	14.6	56.5	22.3	5.1	1.0	0.0
11	Al Asad, Iraq IRQ_ALA	2.0	18.6	39.4	22.8	12.4	4.7	0.0
12	Northern Kuwait KUW_BUE	0.5	11.0	42.0	25.5	10.1	10.8	0.0
13	Central Kuwait KUW_AAS	1.7	38.8	48.8	9.0	1.6	0.0	0.0
14	Coastal Kuwait KUW_SHU	1.1	13.9	29.2	21.9	15.3	18.7	0.0
15	Southern Kuwait KUW_ARI	1.0	17.4	33.6	22.2	16.2	9.7	0.0

It is of note that, except for small percentages in Djibouti and the UAE samples, no particles were recorded in the >15 μm size 'bin'.

DISCUSSION AND CONCLUSIONS

This study characterized three main air-pollution sources: geological dust; smoke from burn pits; and until-now-unidentified lead-zinc smelters and battery-processing facilities. The EPMS has demonstrated the benefits of integrating the analytical results obtained from different measurement techniques into our understanding of the relative contributions of mineral dusts and other aerosols, as encountered at deployment locations within the US Central Command's area of responsibility. This study includes comparative analysis of TSP, PM₁₀, and PM_{2.5} filter samples collected over a period of 1 year. It also includes analysis and comparison to 15 bulk samples from each of the military bases throughout the Middle East (Engelbrecht et al., in press).

Aerosol characterization included chemical analysis by XRF, ICP-MS, ion chromatography, ICP-OES, and thermal optical transmission, mineral analysis by XRD, and individual particle analysis by CCSEM. After validation, all analytical results were compiled on spreadsheets (grouped by sampling site, analytical technique, and chemical species) and posted on the password-protected EPMS webpage maintained by the Desert Research Institute.

Although only about 7% of the days during the 2006–2007 year were sampled on Teflon[®] filters (same percentage for quartz fiber), background levels and areas of concern were identified. Therefore, statistics such as annual averages do not have the same level of confidence as for IMPROVE and CSN monitoring

programs, where both Teflon[®] and quartz fiber filters are sampled on 1-in-3 or 1-in-6 day sampling schedule, giving 33% or 16.7% of the days per year sampled.

Short-term dust events—exacerbated by dirt roads, agricultural activities, and disturbance of the desert surface by motorized vehicles—are largely responsible for the exceeding of particulate-matter annual exposure guidelines and standards (Table 4). The highest annual average for PM₁₀ was recorded at Tallil (303 $\mu\text{g}/\text{m}^3$), followed by Tikrit and central Kuwait. All sites exceed the USACHPPM 1-year air MEG value of 15 $\mu\text{g}/\text{m}^3$ for PM_{2.5}.

By comparison, average PM₁₀ and PM_{2.5} mass and chemical concentration levels from the Middle East deployment sites are—except for a few substances such as nitrate, sodium, and rubidium—as many as 10 times greater than those from five rural (IMPROVE) and five urban (CSN) sites in the southwestern US.

In general, we do not consider dust from studied areas in the Middle East to be out of the ordinary. Comparison of dust samples from the 15 Middle East sites with dust from the US, Sahara, and China shows similar chemical and mineralogical constituents in most cases. Generally, all dust samples contain mixtures of silicate minerals, carbonates, oxides, sulfates, and salts in various proportions. Differences lie in the relative proportions of these minerals and chemical components in different soils. In comparison with the Sahara, China, US, and world dusts, Middle East samples had lower proportions of SiO₂ and higher proportions of CaO and MgO. The last two components are contained in carbonates, such as calcite and dolomite in the soil, more evident in Al Asad and the UAE. Fe₂O₃ and MnO

occur as iron and manganese oxides in greater concentrations in the Sahara, China, and US dust, compared with the 15 Middle East sites.

Dust events subsequently result in short-term elevated levels of soil-forming elements (Figure 7), including magnesium, aluminum, silicon, potassium, calcium, titanium, vanadium, manganese, iron, rubidium, strontium, zirconium, and barium.

Events at Baghdad, Balad, and Taji not corresponding to dust storms resulted in elevated trace-metal concentrations at these sites (Figures 4 and 6). The metals that vary simultaneously with each other (Figure 5) include lead, arsenic, cadmium, antimony, and zinc—all concentrated in the PM_{2.5} size fraction. CCSEM results (Figure 10B) also indicate that lead concentrated in the fine size fraction (0.5–1.0 μm).

In addition to the burn pits, a major potential source of lead and associated zinc, cadmium, arsenic, and antimony in the Baghdad–Balad–Taji region are emissions from secondary lead smelters (<http://www.cpa-iraq.org/business/industries/Battery%20Co.xls>) and related battery-manufacturing facilities affecting the population. As Iraq uses leaded gasoline, vehicle emissions are a contributing source of lead in the atmosphere. Lead from vehicles previously deposited on dirt roads is also continually being re-suspended and may for many years thereafter be a source of aerosol lead. Exploded ordnance also may be a minor contributor of heavy metals in the air during events. Secondary lead-smelting facilities were also reported at Fallujah (<http://minerals.usgs.gov/minerals/pubs/country/2001/izmyb01.pdf>). Lead smelters have been found to be major sources of lead in Cairo's ambient atmosphere (Abu-Allaban et al., 2007). Melting down of old circuit boards and other electronic components for their metal content has been shown to expose communities to extremely high levels of dioxins and metals such as lead, cadmium, and mercury (Carroll & Essik, 2008).

Under fall-to-spring meteorological conditions, heavy-metal pollutants may be trapped within the boundary layer and affect military bases at Baghdad, Balad, and Taji, as well as the Iraqi population living along at least a 75 km stretch of the Tigris River valley.

CCSEM results and secondary electron imagery (Figures 14–16) show that quartz and other silicate minerals and, to a lesser extent, dolomite and calcite particles are coated by a thin Si-Al-Mg layer, probably the clay minerals palygorskite, montmorillonite, and illite. Carbon chains (Figures 13A and 15C) are from combustion sources, possibly diesel vehicle emissions or burn pits.

Further research areas included looking for freshly fractured shards of quartz. Several hundred SEM secondary electron images of individual particles from all 15 sites provided no evidence of such freshly fractured quartz grains. In all instances, quartz grains had rounded edges and were generally coated by clay minerals and iron oxides.

Transmission electron microscope measurements for airborne asbestos were performed on one Nuclepore[®] filter from each site. No asbestos fibers were found.

CCSEM analysis of several million individual particles showed not more than 2.5% carbon by mass on average at any of the sites, with the highest average carbon abundances measured on PM_{2.5} in Bagram and Baghdad.

ENDNOTES

1. US Environmental Protection Agency Quality Assurance Guidance Document 2.12—Monitoring PM_{2.5} in Ambient Air Using Designated Reference or Class I Equivalent Methods, November 1998.
2. National Institute for Occupational Safety and Health (NIOSH) Method 5040—Elemental Carbon (Diesel Particulate), Issue 3 (interim), September 1999.

DECLARATION OF INTEREST

The authors report no conflicts of interest. The authors alone are responsible for the content and writing of the paper.

ACKNOWLEDGEMENTS

We acknowledge contributions by the military public-health soldiers, sailors, and airmen whose efforts were necessary to complete the Enhanced Particulate Matter Surveillance Program (EPMSP). The dedicated effort shown by all participating units in the field, who operated the sampling equipment and collected filter and grab samples, is greatly appreciated. We acknowledge major contributions from the two collaborating laboratories: RTI International, for the filter processing and chemical analysis; and RJ Lee Group Inc. (specifically Traci Lersch), for the CCSEM and SEM individual particle analysis. Thanks are also due to several researchers at DRI who contributed their expertise to the analyses and this report: Michał Skiba for the XRD analysis; Todd Caldwell for analysis of the soil samples; Steve Kohl for the analyses of the re-suspended filter samples, and Dave Campbell for compiling the IMPROVE, CSN, and standards data, and map of the US sampling sites. Finally, the following individuals deserve special recognition for their contributions: Greta Engelbrecht, for data validation, compilation of results, and preparing graphical representations; and James Sheehy and John Kolivosky of USACHPPM, for their support from the inception of the Enhanced Particulate Matter Surveillance Program to its completion. The project was funded under the US Department of Defense contract number W9124R-05-C-0135/SUBCLIN 000101-ACRN-AB.

REFERENCES

- Abu-Allaban, M., Lowenthal, D. H., Gertler, A.W., and Labib, M. (2007). Sources of PM₁₀ and PM_{2.5} in Cairo's ambient air. *Environ. Monitor. Assess.* 133: 417–425.
- Al-Awadhi, J.M. (2005). Dust fallout characteristics in Kuwait: A case study. *Kuwait J. Sci. Engin.* 32:135–151.
- Al-Juboury, A. I. (2006). Authigenic palygorskite in the Middle Miocene rocks of Iraq: Environmental and geochemical indicators. *Geophys. Res. Abstr.* 8: 01584.

- Cagatay, M. N. (1990). Palygorskite in the Eocene rocks of the Dammam Dome, Saudi Arabia. *Clays Clay Min.* 38: 299–307.
- Carroll, C., and Essik, P. (2008). High-tech trash. *Natl. Geograph.* 213: 64–81.
- Clarke, F. W. (1916). *The data of geochemistry*. 3rd ed. United States Geological Survey, Washington, DC.
- Engelbrecht, J. P., Swanepoel, L., Chow, J. C., Watson J. G., and Egami, R. T. (2001). PM2.5 and PM10 Concentrations from the Qalabotjha Low-Smoke Fuels Macro-Scale Experiment in South Africa. *Environ. Monitor. Assess.* 69: 1–15.
- Engelbrecht, J. P., McDonald, E. V., Gillies, J. A., and Gertler, A. W. (2008). *Department of Defense Enhanced Particulate Matter Surveillance Program (EPMSP)*. Desert Research Institute. Report Contract Number: W9124R-05-C-0135/SUBCLIN 000101-ACRN-AB.
- Engelbrecht, J. P., McDonald, E. V., Gillies, J. A., Jayanty, R. K. M., Casuccio, G., and Gertler, A. W. Characterizing mineral dusts and other aerosols from the Middle East—Part 2: Grab samples and resuspensions. *Inhal. Toxicol.* 21: 236–335.
- Goudie, A. S. and Middleton, N. J. (2006). *Desert dust in the global system*. Springer, Heidelberg.
- Kahlaf, F. I., Al-Kadi, A., and Al-Saleh, S. (1985). Mineralogical composition and potential sources of dust fallout deposits in Kuwait. *Sediment. Geol.* 42: 225–278.
- Labban, R., Veranth, J. M., Chow, J. C., Engelbrecht, J. P., and Watson, J. G. (2004). Size and geographical variation in PM1, PM2.5, and PM10: Source profiles from soils in the western United States. *Water Air Soil Poll.* 157: 13–31.
- Yamate, G., Agarwal, S. C., and Gibbons, R. D. (1984). *Methodology for the measurement of airborne asbestos by electron microscopy*. EPA Contract No. 68-02-3266.

Copyright of Inhalation Toxicology is the property of Taylor & Francis Ltd and its content may not be copied or emailed to multiple sites or posted to a listserv without the copyright holder's express written permission. However, users may print, download, or email articles for individual use.